THE ASTROPHYSICAL JOURNAL, **237**:303–318, 1980 April 1

AN OPTICAL STUDY OF THE GIANT RADIO GALAXY NGC 1316 (FORNAX A)

FRANÇOIS SCHWEIZER
Cerro Tololo Inter-American Observatory,[1] La Serena, Chile
Received 1979 June 25; accepted 1979 September 18

ABSTRACT

This paper presents and interprets extensive new photographic, photoelectric, and spectroscopic observations of NGC 1316 obtained with the 0.6, 0.9, 1.5, and 4 m telescopes on Cerro Tololo.

These observations show that NGC 1316 is a typical Morgan D-type galaxy (probably a cD in a poor cluster) with an elliptical-like spheroid embedded in an extensive envelope. There is no dominating exponential disk brighter than $B \approx 26\ \mu$ ($\equiv$mag arcsec^{-2}). The spheroid obeys an $r^{1/4}$ law over distances $\sim$1–50 kpc ($H_0 = 50$), shows color gradients out to at least 30 kpc, and is marked by nonconcentric ripples of 0.1–0.2 mag amplitude that can hardly be in equilibrium. The huge, box-shaped envelope ($\gtrsim 150 \times 220$ kpc) includes various arcs and loops that are probably made up of old stars. From this envelope protrudes a newly-discovered, very faint ($B \approx 27$–$28\ \mu$) but giant ($\sim 110 \times 160$ kpc) loop that is apparently unrelated to the radio lobes. Neither optical-continuum nor Hα-line emission has been detected from the radio lobes themselves.

We report the spectroscopic discovery of a disk of ionized gas that extends out to 54″ (8.5 kpc) from the nucleus. This disk appears to be highly inclined to the stellar spheroid and to rotate much faster ($v \sin i \approx 350$ km s^{-1} versus $\lesssim 80$ km s^{-1}). The well-known central dust lanes are probably associated with the disk and also, we estimate, with at least $3 \times 10^8\ \mathfrak{M}_\odot$ of neutral hydrogen.

An interference-filter search of the galaxy and its radio lobes has yielded a single H II region, which is probably associated with the galaxy.

To explain the inclined gas disk, the presumably tidal perturbations of the galaxy, and the apparent lack of a nearby perturber, we suggest that at least one, and possibly several, gas-rich companion galaxies fell in about 4×10^8–2×10^9 years ago. The resulting infall of gas into the nucleus is likely to have supplied the fuel for past radio outbursts. The presence of two dust lanes that spiral directly into the nucleus suggests that some fueling from the disk continues and further outbursts may be expected.

Other (radio) galaxies with ripples are pointed out, and the companion galaxy NGC 1317 with its two perpendicular bars is briefly described.

Subject headings: galaxies: individual — galaxies: internal motions — galaxies: photometry — galaxies: structure — radio sources: general

I. INTRODUCTION

NGC 1316 (Fornax A) ranks as the fourth-brightest radio source at 1400 MHz and as the third-nearest strong radio galaxy after NGC 5128 (Cen A) and M87 (Vir A). However, unlike the latter two objects, NGC 1316 has been little studied optically, partly because it lacks such distinctive features as the jet of M87 or the massive dust band of NGC 5128, but certainly also because of its southern, −37°, declination. The purpose of the present paper is to provide the basic optical information needed for a deeper understanding of the mechanism that led to the formation of an active nucleus and of two radio lobes.

After the discovery of the radio source by Stanley and Slee (1950), the identification with NGC 1316 was suggested by Shklovskii and Cholopov (1952) and de Vaucouleurs (1953*b*), criticized by Baade and Minkowski (1954), and established unambiguously by Mills (1954) through an improved position measured with his "cross." Wade (1961) discovered that the source consists of two giant lobes separated by 33′ (310 kpc at the 33 Mpc distance adopted below) and each $\sim$20′ (190 kpc) in diameter at half-maximum. A much weaker nuclear source (Cameron 1971) has recently been shown to consist of a compact, subarcsecond core surrounded by an extended component of $\sim$20″ (3.2 kpc) diameter (Geldzahler and Fomalont 1978). Of the three best available radio maps (Lockhart 1971; Cameron 1971; Gardner and Whiteoak 1971), Cameron's is shown in Figure 10 (Plate 12) superposed on a photograph of the galaxy.

Early optical descriptions focused on the inner dust lanes that had suggested already to Evans (1949) a similarity between NGC 1316 (=Arp 154) and NGC 5128 (=Arp 153), and that later guided the identifica-

[1] Cerro Tololo Inter-American Observatory is supported by the National Science Foundation under contract AST 78-27879.

tion with the radio source. Despite the presence of dust, Shklovskii's (1962) hypothesis that the accretion of intergalactic gas by massive spheroidal galaxies might fuel their nuclei and lead to the formation of radio lobes was rejected by Burbidge, Burbidge, and Sandage (1963) because of difficulties that appeared insurmountable at the time. However, the spectroscopic discovery of an inclined gas disk reported in the present paper strongly supports Shklovskii's view.

Later optical work dealt mainly with the outskirts of the giant galaxy. Arp's (1964) discovery of faint extensions toward the radio lobes seemed to provide the missing link between the galaxy and the lobes. Searle (1965) suggested, based on his determination of the rotation axis, that these extensions delineate trailing spiral pathways from the nucleus to the lobes in the fundamental plane of the galaxy. Today, this hypothesis seems tenable no longer. Based on new photographs and our discovery of a truly giant loop of material away from the radio lobes, we are about to argue that the various extensions and loops are *not* directly connected with the lobes, but rather represent the stellar debris caused by the recent infall of one or possibly several galaxies into NGC 1316.

The early controversy over the morphological type and peculiarities of the galaxy was settled elegantly by Matthews, Morgan, and Schmidt (1964), who noted that "the most commonly encountered optical forms of the identified extragalactic radio sources are galaxies having elliptical-like inner regions surrounded by an extensive envelope (the 'D systems' of Morgan's classification)" and classified NGC 1316 as D3–4. Since it is the nearest pure D system in their list (the five times nearer NGC 5128 being classified as intermediate type DE3), a detailed study of this specimen seems important not only in its own right, but also for an improved understanding of the more distant class members. Therefore, two of the main goals of the present study have been to describe the galaxy's morphology from the highest- to the lowest-possible levels of surface brightness and to determine an accurate brightness profile.

Throughout this paper, we adopt a distance of 32.7 Mpc for NGC 1316, based on the recession velocity of 1635 km s^{-1} relative to the Local Group (unpublished measurements; and de Vaucouleurs, de Vaucouleurs, and Corwin 1976 [hereafter 2RC]) and $H_0 = 50$ km s^{-1} Mpc^{-1} (Sandage and Tammann 1976); at that distance 1″ = 158 pc and 10 kpc = 63″. The apparent distance modulus probably approximates the true modulus, $(m - M)_0 = 32.57$, since foreground extinction seems to be negligible at $b^{\rm II} = -57°$ (Sandage 1972*b*). The total visual magnitude, $m_V = 8.77$ (2RC), then corresponds to $M_V = -23.80$.

In the following, we present the observations and data (§ II), describe the morphology of NGC 1316 and of its companion galaxy NGC 1317 (§ III), give brightness and color profiles (§ IV), and discuss the results (§ V). A first-time reader in a hurry may want to glance through § II, familiarize himself with the figures (especially the glossy plates), and then proceed immediately to § V.

II. OBSERVATIONS

The observational data consist of direct photographic plates, photoelectric spot measurements along an east-west axis, and long-slit spectrograms.

Thirty-six direct plates exposed from 10 seconds to 4 hours were obtained in 1976–1978 with the 4 m telescope (18″.6 mm^{-1}) and the Curtis Schmidt telescope (96″.6 mm^{-1}) on Cerro Tololo. Portions of some of the best plates are reproduced in Figures 3–10 (Plates 5–12) with details given in the captions. The bulk of the plates were examined only visually. However, one plate was traced with a microdensitometer to obtain brightness profiles of selected regions, as described in § IV*c*.

To derive photoelectric surface-brightness and color profiles, selected areas of NGC 1316 were observed with the Tololo 1.5 m and 0.9 m telescopes on six nights in 1977–1978. On three of these nights a single-channel photometer was used, and on the remaining nights a three-channel photometer with three-way dichroic beam splitter, which allows simultaneous *UBV* or *UBR* observations, was used. The latter photometer gives increased accuracy for color indices measured on a steeply sloping light distribution. Refrigerated S-20 photomultipliers and pulse-counting electronics were used throughout, and some 12 to 16 standard and extinction stars (Landolt 1973; Crawford, Golson, and Landolt 1971; Johnson $V - R$ from Kunkel and Rydgren 1979) were observed each night.

The selection of areas to be measured presented some difficulties because of the many dust patches in the central region (see Fig. 3); any major- or minor-axis scan crosses several of them. However, inspection of ultraviolet plates shows that the ray from the nucleus due west does not intersect any obvious patch. Therefore, 22 circular areas ("spots") at distances 0″–450″ west along this ray were selected for measurement. The two outermost spots are marked in Figure 1. The aperture diameter varied from 4″.07 near the nucleus to 41″.0 for the outermost spots in order to satisfy requirements of good spatial resolution and signal-to-noise. Overlap observations with different apertures were made at $d_W = 60″$ and 120″. All spots were located at the telescope with an accuracy of $\lesssim 0″.5$ by measured offsets from the nucleus, and two "clean" sky areas at $d_W = 21′02″$ and 26′33″ were frequently monitored by computer-controlled telescope motion.

In order to limit color errors due to differential refraction, measurements with the smallest aperture were rejected unless made at airmass ≤ 1.01 in *U* within 8″ of the nucleus and ≤ 1.04 farther away, ≤ 1.3 in *B*, and ≤ 1.4 in *V* and *R*. The largest airmass observed with the largest aperture was 1.53.

Table 1 gives the averaged *UBVR* data for each spot; all columns except (12) are self-explanatory. Column (12) contains the surface brightness *B* in $\mu \equiv$ mag arcsec^{-2}.[2] Despite the use of various apertures, the conversion from magnitude to surface

[2] *B* magnitudes and *B* surface brightnesses are not distinguished by symbol, but are recognizable from the context or the units (mag or μ).

brightness is believed to have introduced less than 0.005 mag error because the apertures were not only measured micrometrically, but also calibrated relative to each other by observations of the illuminated inside of the dome or the moonlit sky.

Plots of the photometric data are shown in § IV, where the data are discussed.

Finally, a set of long-slit spectrograms was acquired in 1977–1978 with the Ritchey-Chrétien spectrograph of the 4 m telescope. The Carnegie two-stage image tube was used throughout, with gratings giving linear reciprocal dispersions of 25 and 50 Å mm^{-1} at the plate in both the blue and red spectral regions. Exposure times were typically 2–3 hours. Although detailed measurements of most of these spectrograms remain to be done and will be discussed in a later paper, first results based on selected measurements and visual inspection are presented below. Three slit positions for red spectrograms obtained of the outer regions of the galaxy are shown in Figure 1, and eight slit positions for blue spectrograms obtained at different position angles across the nucleus are marked in Figure 11*b*.

III. MORPHOLOGICAL DESCRIPTION

a) *Continuum-emitting Matter*

The appearance of NGC 1316 on photographic plates depends strongly on the exposure, but only weakly on the passband. This indicates changing structure over a wide range of intensities, but rather uniform color. The weakest exposures show a bright nucleus, whereas intermediate exposures emphasize the strong spheroid that is crisscrossed by dust patches and lanes. Deep plates reveal a bewildering variety of extensions in the form of arcs and loops, all apparently immersed in an extensive faint envelope. The following description proceeds from the nucleus to this envelope in order of decreasing surface brightness.

The semistellar nucleus ($\alpha_{1950} = 3^h20^m47^s.209 \pm 0^s.015$, $\delta_{1950} = -37°23'08''.22 \pm 0''.23$ [Schweizer 1980]) is seen on lightly exposed plates from the ultraviolet (Fig. 3, *top left*) to the near-infrared; it appears nearly round, in marked contrast to the elliptical shape of the spheroid ($b/a \approx 0.6$–0.7). As the exposure increases, the nucleus is seen to be bounded to the east by a strong dust lane (§ III*b*). This lane and other, less conspicuous dust make the nucleus appear slightly off-centered toward the northeast with respect to the surrounding spheroid; the effect is most pronounced on ultraviolet and blue plates (Fig. 3, *top right* and *second left*), but barely noticeable in the near infrared. Although ~2.7 mag brighter than the unresolved nucleus of M87 (§ IV*b*), the nucleus of NGC 1316 stands out less because of the different surrounding light distributions; it seems to be merely the central peak of a highly concentrated spheroid, whereas the

TABLE 1

PHOTOELECTRIC *UBVR* DATA FOR 22 SPOTS IN NGC 1316

d_w (arcsec) (1)	Aperture (arcsec) (2)	B (mag) (3)	σ $(0^m.01)$ (4)	U−B (mag) (5)	σ $(0^m.01)$ (6)	B−V (mag) (7)	σ $(0^m.01)$ (8)	V−R (mag) (9)	σ $(0^m.01)$ (10)	n^a (11)	B^b (μ) (12)	$d_w^{1/4}$ (13)
0.0...	4.07	13.80	4	0.60	1	1.02	1	0.91	2	5455	16.59	0.000
2.0...	4.07	14.14	2	0.59	1	1.01	0	0.93	3	4224	16.93	1.189
4.0...	4.07	14.85	2	0.55	4	0.95	3	0.87	4	4223	17.64	1.414
6.0...	4.07	15.40	4	0.52	1	0.97	1	0.84	4	3223	18.19	1.565
8.0...	4.07	15.82	2	0.45	1	0.98	2	0.83	1	2222	18.61	1.682
10.0...	4.07	16.10	4	0.48	1	0.90	2	0.84	1	3223	18.89	1.778
14.0...	4.07	16.47	7	0.46	3	0.93	3	0.80	4	2222	19.26	1.934
18.0...	4.07	16.85	2	0.49	3	0.90	1	0.83	2	4444	19.64	2.060
22.0...	4.07	17.10	-	-	-	-	-	-	-	1---	19.89	2.166
26.0...	4.07	17.36	7	0.41	5	0.90	2	0.81	2	4443	20.15	2.258
30.0...	10.73	15.42	-	-	-	-	-	-	-	1---	20.31	2.340
40.0...	10.73	15.91	1	0.41	3	0.90	1	0.80	1	3332	20.80	2.515
50.0...	10.73	16.34	-	-	-	-	-	-	-	1---	21.23	2.659
60.0...	10.73	16.71	3	0.36	1	0.85	1	0.86	1	3332	21.60	2.783
60.0...	20.22	15.37	-	-	-	-	-	-	-	1---	21.64	2.783
80.0...	20.22	15.98	-	-	-	-	-	-	-	1---	22.25	2.991
100.0...	20.22	16.45	-	-	-	-	-	-	-	1---	22.72	3.162
120.0...	20.22	16.74	2	0.36	12	0.86	1	0.84	1	3222	23.01	3.310
120.0...	41.0	15.22	1	0.40	-	0.84	1	-	-	212-	23.02	3.310
160.0...	41.0	15.78	0	-	-	-	-	-	-	2---	23.58	3.557
200 ...	41.0	16.13	0	0.27	7	0.90	2	0.80	10	4222	23.93	3.761
265[c] ...	41.0	17.11	6	-	-	-	-	-	-	2---	24.91	4.035
350 ...	41.0	17.83	6	-	-	-	-	-	-	3---	25.63	4.325
450 ...	41.0	18.32	26	-	-	-	-	-	-	2---	26.12	4.606

NOTE.- The σ's in columns (4), (6), (8), and (10) are standard deviations of the listed mean magnitudes and colors.

[a] Number of independent observations (i.e., on different nights) averaged in B, U-B, B-V, and V-R.

[b] Surface brightness in $\mu \equiv$ mag $arcsec^{-2}$.

[c] Measured at an offset of 30 arcsec south to avoid two moderately bright stars.

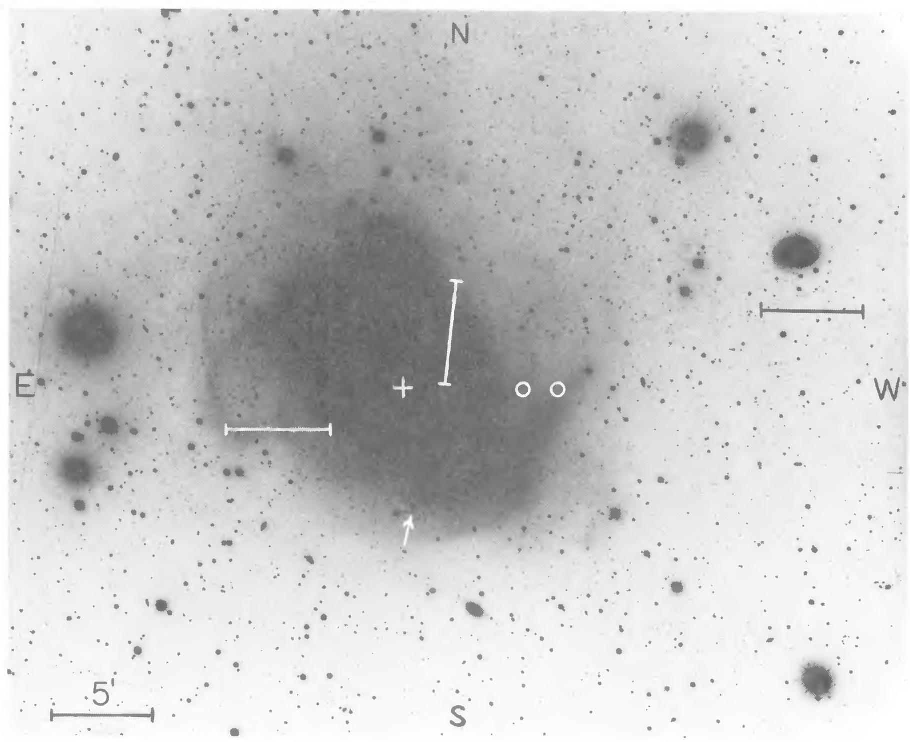

FIG. 1

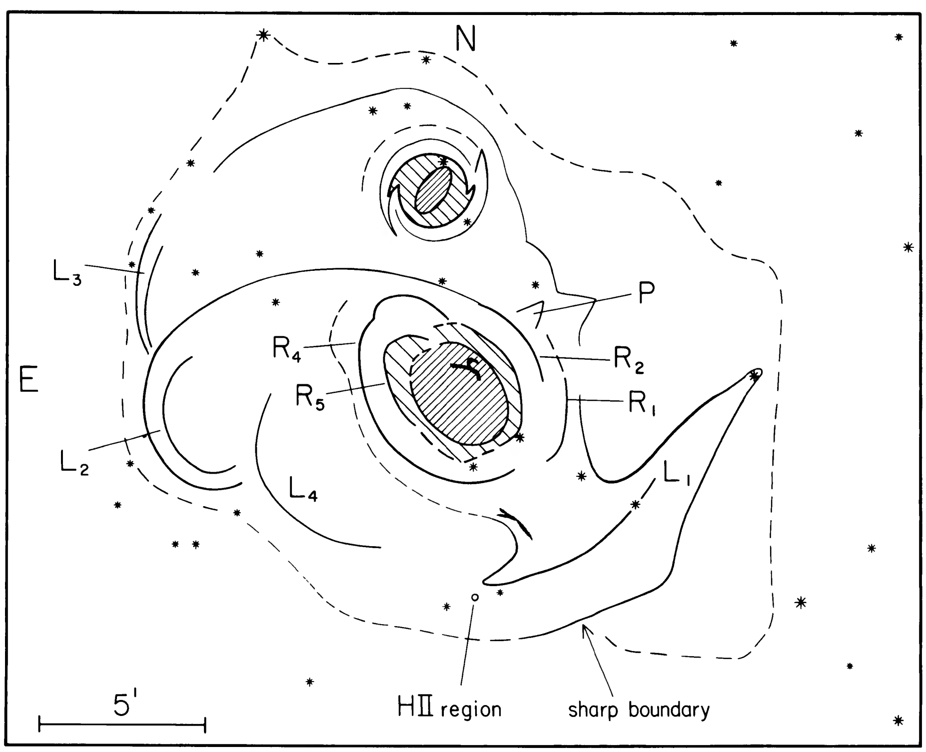

FIG. 2

FIG. 1.—Photoelectric and spectroscopic observations of outer areas of NGC 1316. The cross marks the location of the nucleus. The open circles 350″ and 450″ west of the nucleus indicate the outermost two of 22 spots measured photoelectrically. Three bars mark slit positions of the spectrograph across loops L_2 and L_4 (*horizontal white bar*), plume P and ripple R_2 (*nearly vertical white bar*), and edge of western radio lobe (*horizontal black bar*; spiral galaxy NGC 1310 lies just above). The white arrow points to the only giant H II region discovered in NGC 1316. Compare with Fig. 2.

FIG. 2.—Sketch of structures observed in the spheroid and envelope (*dashed outline*) of NGC 1316: R_1–R_5, ripples (the unmarked R_3 is the next ripple inside R_2); P, plume; L_1–L_4, loops. The two worm-like features (inside hatched area, and NW of H II region) represent major dust lanes. Notice the long arc connecting L_2 with R_2 (cf. with Fig. 6).

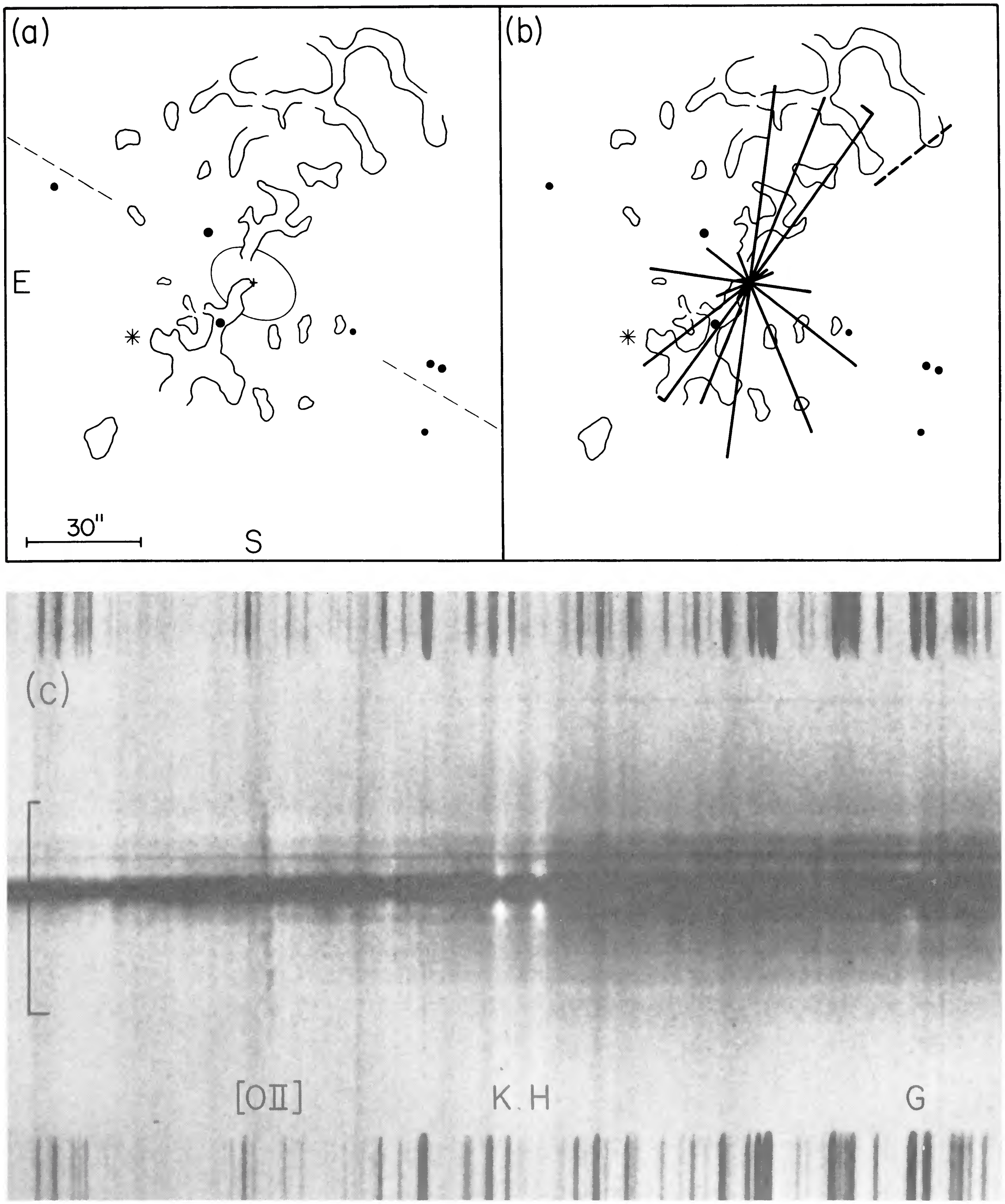

FIG. 11.—Distribution of dust and ionized gas in the central region of NGC 1316. (*a*) Map of dust patches and lanes; the cross, ellipse, and dashed line mark the nucleus, an approximate isophote, and the major axis of the spheroid, respectively. The seven black dots represent the unresolved knots A–G (from west to east). The 30″ scale bar corresponds to 4.7 kpc. (*b*) Distribution of ionized gas; each bar indicates the extent of [O II] λ3727 line emission detected on a spectrogram at that position angle (*dashed*: extremely weak emission). (*c*) Sample spectrogram (4 m tel., 47 Å mm^{-1}, 3 hr) obtained with the spectrograph slit aligned along the minor axis of the spheroid (PA = 142°); southeast is up. The inclined [O II] doublet (unresolved) indicates rapid rotation of the ionized gas, whereas the stellar H and K absorption lines and G band indicate zero rotation for the spheroid. The bar with tick marks at the end shows the extent of line emission and corresponds to the similarly identified bar of frame (*b*). Just above the nuclear spectrum, one sees the streak produced by knot E.

M87 nucleus appears starlike against the large, low-surface-brightness core (Hubble 1923; King 1978; Young *et al.* 1978).

The strong *spheroid* seems to extend from the nucleus to a subjective limit roughly described by an ellipse of semimajor axis $a \approx 4'$, beyond which non-elliptical structures dominate increasingly. The bright inner part of this spheroid shows up well on the (B, 45 s) to (B, 10 min) frames of Figure 3. The apparent axial ratio increases from $b/a = 0.63$ at $a = 30''$ to 0.73 at 2′. The position angle of the major axis is difficult to determine because of the many absorption patches, but it seems to be a rather constant $60° \pm 2°$ within $a = 1'.0$ and it drops irregularly to $51° \pm 2°$ at $2'.5 - 3'.3$ (see also Sérsic's 1968 isophotes). Most striking is the amount of structure that can be discerned in the spheroid on good plates, but that is difficult to reproduce on prints because of the large brightness gradients. We hope that the dodged print of Figure 5 and our sketch in Figure 2 give at least some idea of it. Quite apart from the prominent ripples 2′.5 to 3′.3 WNW of the nucleus that are discussed below, even the spheroid matter within $a \approx 2'.3$ gives the impression of being distributed in *nonconcentric*, *overlapping*, and *only approximate ellipses*. This peculiar distribution probably explains the irregular change of the position angle of the major axis between $a \approx 1'$ and 3′. From comparing several of the plates one gets the further impression that the "bar," which deep plates show protruding to the SW (Figs. 6, 7, and 2), extends in fact through the spheroid to the NE.

The outer part of the spheroid is marked by *ripples*,[3] which show best as elliptical arcs to the NW of the galaxy (R_1 and R_2 in Fig. 2). The dodged print of Figure 5 gives an exaggerated impression of them, whereas the straightforward print in Figure 6 emphasizes their delicate nature (§ IV*c*).

What are the ripples made of? In order to search for possible line emission from the gas that must be associated with the visible dust patches, a 25 Å mm^{-1} red spectrogram was obtained in 2.3 hours with the image-tube spectrograph of the 4 m telescope. The $1''.4 \times 300''$ slit was set at PA = 173°.3 (Fig. 1) across the conspicuous plume P and ripple R_2. Calculations show that even a 10% contribution of Hα line emission to the broad-band light should have been detected easily. No such emission was detected from the ripple or the plume at the 1.2×10^{-17} ergs cm^{-2} s^{-1} arcsec^{-2} level. This suggests that *most of the light in these ripples stems from stars of spectral type later than B0*. An important question to be discussed in § V*d* concerns the structure and origin of these ripples: Are they shells of stars seen edge-on or density ripples in a disk? Are they stable, and what has caused them?

The spheroid is embedded in a huge, roughly box-shaped *envelope* of projected dimensions equaling at least $16 \times 23'$ (150 × 220 kpc; see outermost, dashed contour in Fig. 2). This envelope contains various arc-shaped structures or "loops," the most conspicuous of which have been labeled L_1–L_4 in the figure. Loops L_1 and L_2 appear connected to the spheroid (Arp 1964): L_1 through a bar-shaped extension of the latter, and L_2 through a huge arc of $\sim 10'$ ($\sim$100 kpc) projected length that seems to emerge from ripple R_2 (Figs. 2 and 6). From inspection of deep plates, one gets the impression that L_1 may itself be a loop seen at high inclination. As in the ripples, most of the light in the loops probably stems from stars. A 3 hour spectrogram obtained with the 4 m spectrograph slit aligned at PA = 90° on the southern part of L_2 (Fig. 1) shows, again, no sign of Hα emission. It is very difficult to judge whether the structure of the loops is knotty or not, because of the vast number of background galaxies seen on the deepest IIIa-J plates exposed at prime focus. To us, loops L_1–L_4 *appear* smooth, which would indicate a stellar population of at least intermediate age ($\gtrsim 10^8$ yr).

To the SSW, the envelope appears sharply bounded (Figs. 2, 7, and 8) in a manner reminiscent of the tidal cutoffs seen in strongly interacting galaxies (e.g., the western edge of NGC 5194 [Burkhead 1978; Toomre 1978]). However, even beyond this boundary there is luminous material. On deep IIIa-J plates obtained with the Curtis Schmidt telescope, we discovered a gigantic broad loop of exceedingly low surface brightness (estimated $B \approx 27$–$28\ \mu$) and $\sim 12' \times 17'$ ($\sim$110 × 160 kpc) outer dimensions; it is shown in Figure 9 on integration prints of five of the plates and henceforth will be referred to as loop L_5. Its reality is beyond question: it is seen not only on plates centered at different points, thus excluding the possibility of its being an internal reflection, but also on the film copy of field No. 301 of the SRC (J) sky survey.[4] As far as its faintness allows one to judge, the loop seems to emerge from the region of the barlike extension of the spheroid and to fade just as it returns to the envelope farther east. Slightly NE of its southern tip, it shows structure in the form of two fuzzy patches seen weakly in Figure 9. On a IIIa-J plate taken of this region with the 4 m telescope, especially the fainter, northern fuzz shows resolution into four knots, two of which appear near stellar. They may well be groups of early type stars, and weak Hα might be detectable spectroscopically.

On none of our plates or integration prints can we detect any extended source of optical radiation corresponding to the radio lobes (Fig. 10) down to an estimated surface brightness of $B \approx 28\ \mu$. The only apparent coincidence is that loop L_1 protrudes into a "valley" of the radio map of the western lobe; but, given the likely stellar nature of L_1, this coincidence seems fortuitous.

b) Dust

The dust patches in the spheroid are so pronounced (Fig. 3) that Shapley seems to have mistaken them for

[3] These ripples were first pointed out to me by Dr. John A. Graham on a plate obtained by him in 1975.

[4] Dr. J. A. Graham communicates that this loop has been discovered independently by Mr. D. F. Malin of the Anglo-Australian Observatory.

plate defects (Hodge 1975). They are arranged with some degree of symmetry relative to the nucleus and seem to form two systems, one to the NW and the other to the SE (see also Fig. 11a). On weakly exposed blue plates, two radial dust lanes are prominent that lead to the nucleus from opposite sides and look like umbilical cords. The SE lane can be traced to within 0"9 (140 pc) of the center and seems to reach the nucleus from the near side, whereas the NW lane fades several arcseconds from the center and apparently reaches the nucleus from the far side. This impression of near and far is conveyed by the much better visibility of the SE lane within 14" (2.2 kpc) from the nucleus. At about this distance, the lanes break up into various patches whose relative visibility reverses beyond, the NW patches now being more prominent and extending farther out. If we interpret the changing relative visibility as due to the changing depth of the dust within the stellar system, it implies that the dust either follows some spiral path in a plane inclined to the equator of the spheroid or else has some three-dimensionally twisted distribution. At 25"–30" (4–5 kpc) from the center, the predominant orientation of the various patches and lanes changes from radial to azimuthal, giving the dust, according to Burbidge, Burbidge, and Sandage (1963), a distribution vaguely reminiscent of spiral arms.

A lower limit to the amount of H I gas associated with this dust can be estimated as follows: The filaments of the NW system that are apparently optically thick cover about 490 square arcseconds (1.2×10^7 pc^2). Under the assumptions that (i) their gas-to-dust ratio is similar to that in our own Galaxy, with $N_{\rm H\,I}/E_{B-V} \approx 5.1 \times 10^{21}$ cm^{-2} mag^{-1} (Knapp and Kerr 1974; Jenkins and Savage 1974; and Heiles 1976), and (ii) their optical depth is at least unity, we find $\mathfrak{M}$(H I, NW) $\gtrsim 1.3 \times 10^8\, \mathfrak{M}_\odot$. Since the less visible SE system probably is of comparable strength, the total mass of H I within the spheroid alone is likely to exceed $2.6 \times 10^8\, \mathfrak{M}_\odot$.

However, the presence of dust is not restricted to the spheroid. Individual dust patches can still be seen out to ~2'.3 (22 kpc) along the minor axis, in the region of ripple R_2 (Fig. 5). Also, a ~1'.1 (10 kpc) long string of dust lanes is prominent near the SE border of the barlike extension at 4'.6 (44 kpc) to the SW of the center. Thus, the total amount of H I associated with NGC 1316 is likely to substantially exceed $3 \times 10^8\, \mathfrak{M}_\odot$.

c) *Ionized Gas and Young Stars*

The presence of a small amount of ionized gas in the nucleus is revealed by weak emission lines of [O II] λ3727, [N II] λ6583, and [S II] λλ6716, 6731 (interval λλ4500–5700 not observed). On spectrograms of 25 Å mm^{-1} dispersion, the [O II] doublet appears unresolved and the [N II] line broadish, which seems to indicate a moderate amount of turbulence in the gas. The [S II] lines are just weakly detected against the stellar continuum, whereas Hα is lacking, buried perhaps in a weak stellar absorption line. Otherwise, the nuclear spectrum is marked by the strong absorption lines typical of the old population in giant ellipticals (Ca II H + K, G-band, Na D). Apparently, the nucleus of NGC 1316 is now fairly inactive.

Outside the nucleus, the distribution of [O II] λ3727 and [N II] λ6583 line emission indicates the existence of *an extended and probably disk-shaped region of ionized gas* with a maximum projected radius of at least 54" (8.5 kpc) at PA = 322°. Figure 11*b* depicts the observed distribution as inferred from the maximum extent of the [O II] doublet on a set of eight uniformly exposed 4 m spectrograms obtained at different position angles (47 Å mm^{-1}, 2–3 hr each). Obviously, the distributions of ionized gas and dust are similar.

The kinematics of the gas revealed by visual inspection of these spectrograms is both unexpected and intriguing, as can be seen from the sample spectrogram shown in Figure 11*c*. Whereas the stellar spheroid rotates slowly even along its major axis ($v \sin i \lesssim 80$ km s^{-1} out to 30" [4.7 kpc]),[5] the gas shows rapid rotation with a maximum velocity gradient at PA = 127°–142°, i.e., roughly *along the minor axis of the spheroid.* This is also the direction of maximum extent of the gas. Relative to the nucleus, the SE side of the presumed disk approaches, whereas the NW side recedes, with velocities of up to about ∓350 km s^{-1} at the detection limits 35" SE and 54" NW. Although only the detailed measurements will show to what extent the motions of the ionized gas can be represented by pure rotation, it seems clear already from this preliminary evidence that the projected rotation axes of stars and gas are roughly perpendicular.

A search for H II regions in NGC 1316 and the radio lobes was made on two sky-limited plates exposed at the 4 m prime focus through an Hα interference filter (90 Å FWHM) optimized for 1800 km s^{-1} redshift. Both plates were of the same 46' × 46' field; one was exposed for 3¾ hr on baked 127-04 emulsion, the other for 2¼ hr on baked 098-04 emulsion. A single H II region was discovered, which lies 6'.7 (63 kpc) south of the nucleus (Figs. 1, 2, and 6). The main Hα emission comes from a banana-shaped, 1".5 × 3".5 (240 × 550 pc) region along the southwestern edge of a round blue fuzz of 5".6 (880 pc) diameter. The latter probably is an associated complex of OB stars. The line-of-sight velocity relative to the nucleus of NGC 1316 is only -105 ± 8 km s^{-1}, as measured from a 25 Å mm^{-1} spectrogram. Therefore, the region is probably gravitationally bound to the galaxy and orbits like the gas or stars. Why only this one giant H II region should have been formed remains mysterious, but we note that there is a 10 kpc long dust lane "nearby" (§ III*b*) that probably signals the presence of large-scale shocks in the gas (Fujimoto 1966; Roberts 1969).

Can weak optical emission lines be detected from

[5] Our spectrograms confirm Searle's (1965) conclusion that maximum rotation occurs roughly at the major axis (PA ≡ 60°), but show unambiguously that it is the *southwest* side that approaches, not the northeast side as stated by Searle.

the radio lobes? To answer this question, we obtained a red spectrogram (50 Å mm^{-1}, 2 hr) with the slit of the 4 m image-tube spectrograph put across the steep outer gradient of the western lobe, 3′ to the south of NGC 1310 (cf. Figs. 1 and 10); the 1″.4 × 5′ slit extended from the peak of the lobe westward to about half-peak radio brightness. We hoped that there might perhaps be a detectable amount of ionized gas at the interface between the relativistic plasma and the surrounding medium, in analogy to supernova remnants. However, no Hα line emission was detected, with an upper limit of 0.9 (±0.2) × 10^{-17} ergs cm^{-2} s^{-1} $arcsec^{-2}$. This flux limit implies an electron density $n_e \lesssim 5 \times 10^{-3}$ cm^{-3} if one assumes, admittedly somewhat artificially, that the lobe is a sphere uniformly filled with optically thin gas radiating at $T = 7000$ K (see Osterbrock 1974). The limit for n_e is seven orders of magnitude higher than the number density of *relativistic* electrons estimated from the observed synchrotron radiation ($n_{e,\mathrm{rel}} \approx 10^{-10}$ cm^{-3}; Moffet 1975). A further search across the *outer* isophotes of the lobes still seems worthwhile, especially if the sensitivity can be improved by an order of magnitude.

In summary, ionized gas has been detected (i) in the nucleus, (ii) in a disk of similar extent as the dust patches and that apparently rotates at a ~90° angle to the spheroid, and (iii) in one giant H II region. Direct evidence for young stars has been found so far only in the blue fuzz associated with this H II region. No extended Hα emission or Hα hot spots have been seen on three spectrograms covering loop L_2, ripple R_2 plus plume P, and the western radio lobe, respectively.

d) (*Globular?*) *Clusters*

Deep IIIa-J plates of NGC 1316 appear so crowded with faint galaxy images that we have found it impossible to identify any globular clusters in the outskirts. However, on short-exposure plates one notices a significant excess of faint, stellar-looking images ("knots") within a 1′ radius of the nucleus (Fig. 3); the seven brightest are indicated as black dots in Figure 11*a* and named A–G in order of increasing right ascension. We estimate apparent magnitudes $B \approx 19\frac{1}{2}\,(-\frac{1}{2}, +1)$ for knot E and $B \gtrsim 20$ for all others by approximate photographic comparison with an unpublished photoelectric sequence 10°.2 away. The main uncertainty in the magnitudes stems from the corrections for galaxy background. The corresponding absolute magnitudes for zero extinction, $M_B = -13\ (-\frac{1}{2}, +1)$ and $M_B \gtrsim -12\frac{1}{2}$, seem slightly too bright for globular clusters (cf. with $M_B \approx -10.5$ in M31 [van den Bergh 1969] and −11.2 for cluster I-40 in M87 [Racine, Oke, and Searle 1978)]. However, inspection of ultraviolet to near-infrared plates shows these knots to have colors similar to those of the spheroid itself, thus rendering it unlikely that they are young OB associations. Also, streaks made by knot E on two blue spectrograms taken at PA = 142°, with the knot riding on the slit edge (cf. Figs. 11*b* and 11*c*), show no signs of λ3727 or Balmer emission, but seem to show H + K absorption lines and the G band at roughly the redshift of the galaxy background (about 200 km s^{-1} less). Hence, it also seems improbable that knot E is a galactic foreground star. At least that knot seems to be a bright (globular?) cluster in NGC 1316, and several of the others may be likewise.

e) *Morphology of the Companion Galaxy NGC 1317*

Because NGC 1317 appears on all plates obtained of NGC 1316 and may be physically associated, we briefly describe its morphology. Figure 4 shows the galaxy on six plates of different exposure.

The nucleus of the companion ($\alpha_{1950} = 3^h20^m 49^s.664 \pm 0^s.015$, $\delta_{1950} = -37°16'51''.95 \pm 0''.16$ [Schweizer 1980]) is less bright than that of NGC 1316, more fuzzy, and contrasts less with the surroundings. On ultraviolet and blue plates taken in 1″ seeing, the peak surface brightness is about 5 ± 1 times lower than in NGC 1316.

Surrounding this nucleus is a 14″ (2.2 kpc) long bar oriented at PA = 58°.1 ± 0°.6. At its ends, the bar is bounded in classical fashion (Sandage 1961) by an elongated lens of $b/a = 0.82$.

An elliptical ring of H II regions and OB associations prominent on UV plates encircles lens and bar. It has a semimajor axis of 13″ (2.0 kpc) and is more elongated ($b/a = 0.76 \pm 0.02$) than the lens. The ring appears broken at PA ≈ 80° and 315° by two dust lanes that originate near the ends of the bar and wind into the outer body of the galaxy. Preliminary study of spectrograms obtained at different position angles shows that the ring rotates with a maximum approach velocity $v \sin i = -68 \pm 11$ km s^{-1} at PA = 36° ± 5°.

A second, "fat" bar of ~60″ × 80″ (9.5 × 12.7 kpc) dimensions is visible on long exposures (Fig. 4; frames [*B*, 40 min] and [*B*, 105 min]), with two indentations at PA ≈ 45° and 225° created by the above-mentioned dust lanes. This bar is aligned at PA = 148°.4 ± 0°.9, perpendicularly (90°.3 ± 1°.1) to the small inner bar. Since NGC 1317 appears nearly face-on, the two bars are probably also perpendicular in space. Bars within bars have been noticed in two galaxies before (de Vaucouleurs 1974), but this seems to be the first perpendicular pair known.

The "fat" bar itself is embedded in a disk that contains many dust lanes and faint blue knots. Two broad spiral arms of low surface brightness emerge from this disk and connect to two even fainter spiral structures of small pitch angle (best seen on Fig. 6).

The companion NGC 1317 has been classified SAB(rs)a pec in the 2RC, but seems to us to be a very late SB(rs)a or early SB(rs)b in the Hubble classification (Sandage 1961) because of the two dust lanes that spiral from the ends of the inner bar over 240° into the outer disk. Note that despite its apparent proximity to NGC 1316 (projected separation 6′.3 = 60 kpc) and small relative velocity (+171 ± 5 km s^{-1} [unpublished]), NGC 1317 *looks* very regular and unperturbed.

IV. PHOTOMETRIC PROPERTIES

a) East-West Brightness and Color Profiles

The photoelectric measurements of blue surface brightness (Table 1, col. [12]) are plotted twice in Figure 12. The left panel is a plot of B versus *linear* distance west (d_W), in which an exponential disk (Patterson 1940; de Vaucouleurs 1959; Freeman 1970) would be represented by a straight line. As that panel shows, there is no such line and therefore no dominating exponential disk in NGC 1316 out to 450″ (71 kpc) west. On the other hand, the right panel, which is a plot of B versus $d_W^{1/4}$, shows that the data obey the $r^{1/4}$ law characteristic of elliptical galaxies (de Vaucouleurs 1953a; Kormendy 1977) over distances from ~6″ to at least 350″ (1–55 kpc) west. Thus, *in its main body NGC 1316 unquestionably is a giant elliptical galaxy*.

Remarkably, the $r^{1/4}$ law seems to apply well beyond the subjectively defined spheroid ($d_W \lesssim 220''$) into the inner envelope. Even the outermost measurement at 450″ west does not deviate from the law by more than its rather large error ($\sigma = 0.26$). However, since the measured area contains part of loop L_1 (Fig. 1), a significant brightness excess there and beyond would be expected with measurements of higher accuracy.

To get a feel for the deviations from an exact $r^{1/4}$ law, we made a linear least-squares fit to the 18 data points within $6'' \leq d_W \leq 350''$ and obtained

$$B = 14.12(\pm 0.07) + 2.668(\pm 0.026) d_W^{1/4} , \quad (1)$$

with a mean residual of 0.09 mag per point. This fit is drawn in Figure 12*b* as a dashed line and appears satisfactory. However, residuals show a systematic, wavelike pattern with amplitudes of up to 0.22 mag that are significantly larger than the measuring errors. Similar wavy residuals have been observed in NGC 3379 (de Vaucouleurs and Cappacioli 1979), yet their meaning is not understood since the $r^{1/4}$ law itself lacks a physical explanation. On the admittedly arbitrary assumption that at least the positive deviations (in terms of flux) may represent parts of a fragmentary disk within the spheroid, the residuals place an upper limit of ~20% on the fractional light contribution from that disk at any distance between 1 and 55 kpc west.

Color profiles measured photoelectrically out to 200″ west are shown in Figure 13, with *UBVR* indices taken from Tables 1 and 2. Corrections for redshift have been neglected since they are $\lesssim$0.01 mag (Schild and Oke 1971; Whitford 1971; Sandage 1972*a*). The color indices are typical of a giant elliptical (de Vaucouleurs and de Vaucouleurs 1972; Sandage 1972*a*), as was already known from the integrated values $(U - B)_T = +0.49 \pm 0.04$ and $(B - V)_T = +0.90 \pm 0.03$ given in the 2RC. All profiles indicate marked color gradients within the central 10″ (1.6 kpc) of NGC 1316, the nucleus being reddest. Weaker gradients can be detected out to the observational limit at 200″ (32 kpc) west in the indices that contain the ultraviolet, especially in $U - R$.

These color gradients are probably caused mainly by abundance variations, rather than internal reddening,

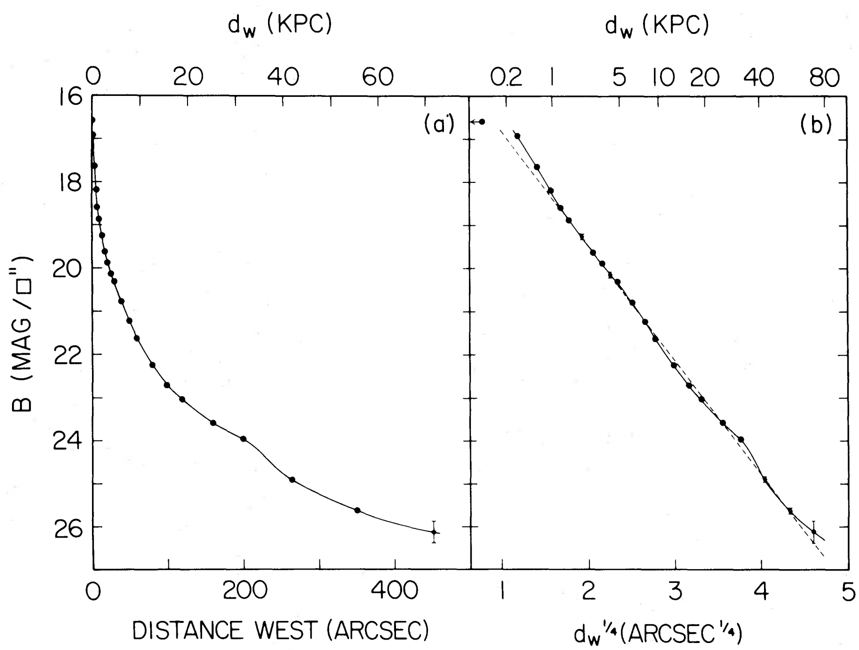

FIG. 12.—Photoelectrically measured brightness profile of NGC 1316 from the nucleus westward. Data points represent the mean surface brightness B in small diaphragms; solid lines are drawn by hand. (*a*) A plot of B as a function of linear distance shows no straight-line segment, which means there is no dominating exponential disk. Only the largest error bar is drawn. (*b*) A plot of B as a function of $d_W^{1/4}$ shows the $r^{1/4}$ law characteristic of elliptical galaxies. Error bars are given for the five points with $\sigma_B > 0.04$ mag. The dashed line represents the least-squares fit of equation (1).

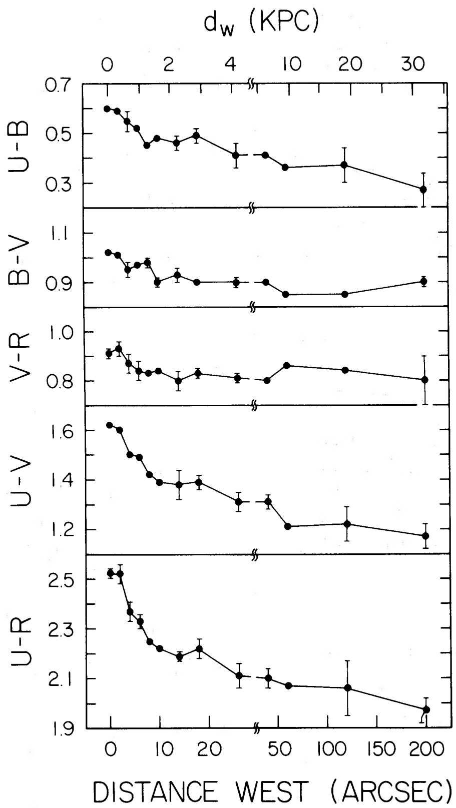

FIG. 13.—Photoelectrically measured color profiles of NGC 1316 from the nucleus westward. Points without error bars have $\sigma < 0.02$ mag. Note that the horizontal scale changes by a factor of 5 at $d_W = 30''$. Color gradients are especially pronounced in $U - V$ and $U - R$ and probably reflect abundance gradients.

for two reasons: (i) The measured areas contain no absorption patches detectable even on ultraviolet plates. (ii) Other giant ellipticals without known dust patches often show similar color gradients (Strom and Strom 1978) that are generally attributed to abundance variations (Strom *et al.* 1976; Aaronson *et al.* 1978; Sandage and Visvanathan 1978). Hence, with the aid of calibration relations given in these references, we have converted the $U - B$ and $U - V$ indices to logarithmic metal-to-hydrogen ratios relative to the Sun. These ratios, listed in the last two columns of Table 2, suggest that the metallicity of NGC 1316 decreases from slightly more than twice solar at the center to about 40% solar at 32 kpc west. For a detailed discussion of the uncertainties, consult the references above.

b) *The Nucleus*

Figure 12*b* shows that at distances of $\sim 1''$–$6''$ (0.16–1.0 kpc) from the nucleus the blue surface brightness observed photoelectrically exceeds that expected from the extrapolated $r^{1/4}$ law. This brightness excess is confirmed by high-resolution photographic photometry, the details of which will be reported elsewhere (Schweizer 1980). Here we simply summarize the main results.

The *apparent* core radius (=half width at half-maximum [see Schweizer 1979]) of NGC 1316 is very small and depends on the seeing: $1\overset{''}{.}60 \pm 0\overset{''}{.}1$ in $0\overset{''}{.}88$ (HWHM) seeing and $1\overset{''}{.}04 \pm 0\overset{''}{.}1$ in $0\overset{''}{.}53$ (HWHM) seeing. Nevertheless, the nucleus is clearly *not* a point source, as confirmed by fitting various seeing-convolved models to the observed profiles. This agrees with the observation that the blue spectrum resembles that of an old stellar population and lacks an appreciable nonthermal component (§ III*c*).

The *intrinsic* core radius obtained from best fits with an isothermal sphere is $r_c \lesssim 0\overset{''}{.}6$ (100 pc), and the intrinsic central surface brightness $B \lesssim 13.9\mu$. The integrated apparent magnitude of the core is $B_c = 14.7 \pm 0.5$ mag, or about 2.7 mag brighter than that of the unresolved spike in M87 (Young *et al.* 1978), and corresponds to $M_B = -17.9 \pm 0.5$ or 2.3×10^9 $L_{B,\odot}$ (blue solar luminosities). The blue volume luminosity and mass density, both averaged over the core, are at least $140\, L_{B,\odot}\, \mathrm{pc}^{-3}$ and $800\, \mathfrak{M}_\odot\, \mathrm{pc}^{-3}$, respectively.

c) *The Ripples*

To estimate the brightness enhancements in the prominent ripples R_2 and R_4, tracings were made of plate P-3411 (Fig. 5) with the CTIO Grant microdensitometer. The scans started at the nucleus and crossed R_2 at 172″ from the nucleus and position angle 298° and R_4 at (196″, 61°), where the labeling lines in Figure 2 nearly touch the ripples. Figure 14

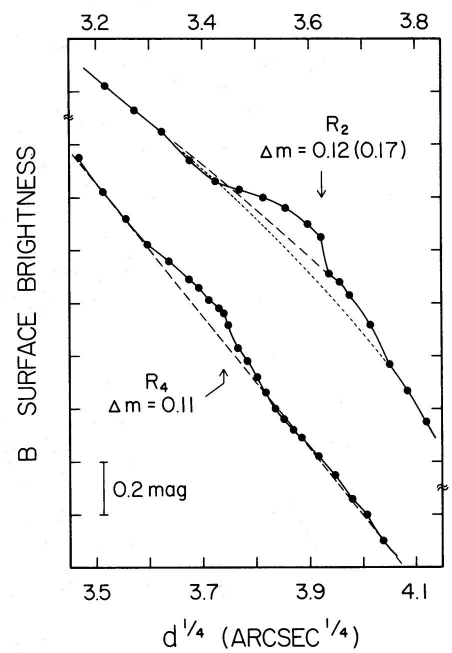

FIG. 14.—Photographically measured blue brightness profiles through the two prominent ripples R_2 and R_4. The brightness zero point is arbitrary, and *d* is the distance from the nucleus. Data points represent the measurements, solid lines are drawn by hand, and dashed lines mark estimated galaxy backgrounds (two possibilities shown for R_2). The arrows indicate the ripple boundaries seen on the plate and are labeled with the magnitude difference above background.

TABLE 2

PHOTOELECTRIC *UBVR* COLORS AND METALLICITIES IN 13 SPOTS OF NGC 1316

d_w^a (arcsec)	d_w^a (kpc)	U-B	σ (.01)	U-V	σ (.01)	U-R	σ (.01)	$[M/H]^b_{U-B}$	$[M/H]^c_{U-V}$
0.0...	0	0.60	1	1.62	0	2.52	2	+0.24	+0.42
2.0...	0.32	0.59	1	1.60	1	2.52	4	+0.22	+0.38
4.0...	0.63	0.55	4	1.50	1	2.37	4	+0.14	+0.21
6.0...	0.95	0.52	1	1.49	1	2.33	3	+0.08	+0.20
8.0...	1.27	0.45	1	1.42	0	2.25	0	-0.06	+0.08
10.0...	1.6	0.48	1	1.39	1	2.22	1	0.00	+0.02
14.0...	2.2	0.46	3	1.38	6	2.19	2	-0.04	+0.01
18.0...	2.8	0.49	3	1.39	3	2.22	4	+0.02	+0.02
26.0...	4.1	0.41	5	1.31	4	2.11	5	-0.14	-0.11
40.0...	6.3	0.41	1	1.31	3	2.10	4	-0.14	-0.11
60.0...	9.5	0.36	1	1.21	0	2.07	1	-0.24	-0.28
120.0...	19.0	0.37	7	1.22	7	2.06	11	-0.22	-0.27
200.0...	31.6	0.27	7	1.17	5	1.97	5	-0.42:	-0.39

[a] Distance west of nucleus.

[b] Logarithmic metal-to-hydrogen ratio relative to the sun, inferred from U-B with relations given by Strom et al. (1976).

[c] Same, but from U-V with relations by Aaronson et al. (1978).

shows the resulting profiles of blue surface brightness versus the fourth root of the distance. Ripple R_2 appears superposed on the slightly bumpy background of the galaxy. Depending on how one chooses to interpolate (two dashed lines), the contrast Δm of this ripple over the background ranges between 0.12 and 0.17 mag. On the other hand, the background of ripple R_4 is well represented by the $d^{1/4}$ law (*dashed line*) and the contrast is $\Delta m = 0.11$ unambiguously. Thus the profiles show that two of the most prominent ripples represent 0.1–0.2 mag enhancements in blue surface brightness over the galaxy background.

The corresponding enhancements in surface mass density are 10–20%, if the stellar populations in the ripples have a similar mass-to-light ratio as the background. However, if the ripple populations are younger and have a lower $\mathfrak{M}/L_B$, then the density enhancements may be significantly less.

V. DISCUSSION

The goal now is to fit the various observed features into a coherent picture. Two questions are of foremost interest: What made NGC 1316 erupt as a radio galaxy? And what relations exist between the current optical structure and the radio lobes?

The discussion below proceeds from well-established results to more and more speculative conclusions.

a) *A Typical D Galaxy*

The brightness and color profiles (Figs. 12 and 13) establish beyond doubt that within at least 50 kpc radius NGC 1316 is essentially an elliptical. On the other hand, visual inspection of the various photographs (esp. Fig. 8) clearly shows the presence of an extended envelope with structure and nonelliptical isophotes. Therefore, NGC 1316 indeed fits Morgan's description of a D galaxy (§ I).

Earlier classifications of NGC 1316 as an S0 or even Sa galaxy (Baade and Minkowski 1954), made presumably because of the presence of dust, were clearly mistaken. There simply is not any substantial exponential disk brighter than $B \approx 26\ \mu$.

The extent to which the $r^{1/4}$ law fits the data far into the subjectively defined envelope is perhaps surprising. Deviations from the law larger than ~0.2 mag occur only at $B \approx 26\ \mu$, the limit of our photometry, and presumably increasingly below. However, this result agrees with Oemler's (1973, 1976) observations of cD galaxies, which show that the envelopes set in typically at $B \approx 24$–$26\ \mu$.

The small core radius (§ IV*b*) of this giant galaxy is more startling, especially when compared to the substantially larger core radii of 16 less luminous ellipticals observed by King (1978). Oemler (1976) seemed to find a positive correlation of core radius with luminosity. However, his sample consisted of significantly more distant galaxies, whose core radii may be severely affected by seeing (Schweizer 1979). Therefore, it seems difficult at present to judge whether NGC 1316 is abnormal in this respect or not; it certainly lacks the double or multiple nuclei found in a fair fraction of D galaxies (Matthews, Morgan, and

Schmidt 1964). Yet, arguments to be presented in § V*c* suggest that NGC 1316 may *temporarily* have had more than one nucleus in the not too distant past.

Is NGC 1316 peculiar for a D galaxy? The presence of dust can barely be called peculiar: increasingly often, dust is found in spheroidal galaxies misclassified as S0's precisely because of its presence, and in radio galaxies dust is in fact quite common (Kotanyi and Ekers 1979). The gas disk itself can barely be termed peculiar either, partly because gas is to be expected wherever dust occurs, but also because similar gas disks have already been discovered in various ellipticals (§ V*b*). Perhaps the most peculiar attributes of NGC 1316 are the loops in the envelope. However, even they may be common and may simply not yet have been found in more distant D systems because of seeing limitations and lesser observational effort. The majority of the D galaxies illustrated by Matthews, Morgan, and Schmidt (1964) do, in fact, show distinct envelope asymmetries that with increased resolution may turn out to be loops. Thus, with the possible exception of its small nucleus, NGC 1316 appears to be a *typical* D galaxy.

What is its environment? Figure 15 shows that the galaxy is located on the outskirts of the Fornax I cluster, about 3°.3 or one cluster radius (Zwicky 1959; de Vaucouleurs 1975; Welch, Chincarini, and Rood 1975) to the southwest of the center. NGC 1316 is the brightest galaxy in the area, 0.8 visual magnitudes brighter than the barred spiral NGC 1365 to the northeast and 1.1 mag brighter than NGC 1399, the brightest elliptical in the cluster core (2RC). This high luminosity and, by inference, high mass, coupled with the peripheral position, suggest that NGC 1316 and the small galaxies near it form a separate dynamical entity. (For this reason, we adopted in § I a distance based on the galaxy's redshift rather than on the mean cluster redshift.) If this view is correct, NGC 1316 belongs to the class of D and cD galaxies in poor clusters (Morgan, Kayser, and White 1975; Albert, White, and Morgan 1977) and lies ~ 5 Mpc beyond the Fornax I cluster.

Also, NGC 1316 may then have to be called a cD galaxy because of its 2.2 mag brightness excess over the brightest neighbor, NGC 1317. This cD classification would agree with the absolute magnitude $M_V = -23.8$ (§ I), which is brighter than observed for six D and 13 cD galaxies in poor clusters (Schild and Davis 1979) and which fits into the range $-23.5 \leq M_V \leq -26.0$ for cD's in rich clusters (Oemler 1976).

b) *Infall of Gas*

The presence of an extensive disk of gas that rotates much faster than the stellar spheroid and around a different axis (§ III*c*) leaves little doubt about its origin: it must consist of gas that fell in rather recently. Gas shed by the stars of the spheroid could not have picked up the observed angular momentum, either by amount or in direction. On the other hand, gas fallen in long ago would probably have precessed and, because of the dissipative nature of collisions between gas clouds, would have settled into the fundamental plane of the spheroid after a few revolutions. Therefore, it seems likely that the gas fell in less than 10^9 years ago.

NGC 1316 is about the fourth case of a spheroidal galaxy known to have an inclined gas disk. Previously known were NGC 1052 and 4278, where gas rotates at $\sim 50°$ to the spheroids (Fosbury *et al.* 1978; Knapp, Gallagher, and Faber 1978; Reif, Mebold, and Goss 1978; Knapp, Kerr, and Williams 1978), and NGC 2685, where two different gas rings coexist, one apparently aligned with the spheroid and the other at a right angle (Ulrich 1975; Shane 1977; Schechter and Gunn 1978). In a few other cases, a rotating gas disk has been detected, but the rotation axis of the spheroid remains unknown, as, e.g., in NGC 4636 (Knapp, Faber, and Gallagher 1978; Bottinelli and Gouguenheim 1978) and NGC 5128 (Burbidge and Burbidge 1959; Graham 1979). Remarkably, three of the five mentioned galaxies also share with NGC 1316 the property of having a compact radio core: NGC 1052, 4278, and 5128. Therefore, NGC 1316 seems to be but one specimen in the growing class of ellipticals with inclined disks of gas and strong nuclear radio emission.

c) *Infall of One or Several Galaxies*

Infall of gas alone does not seem sufficient to explain the various perturbations observed in NGC 1316. The loops, ripples, and sharp southwestern boundary all convey the impression that the galaxy has been damaged tidally, an impression further supported by evidence that the loops and ripples consist of older stars (§ III*a*). To produce such damage, an infalling gas cloud would have had to be not only compact but also massive ($> 10^{10}\, \mathfrak{M}_\odot$) since NGC 1316 itself has a mass of the order of $2 \times 10^{12}\, \mathfrak{M}_\odot$ (for an assumed $\mathfrak{M}/L_B = 10$). However, intergalactic clouds of $10^{10}\, \mathfrak{M}_\odot$ have never been found despite various searches (e.g., Sargent 1977; Materne, Huchtmeier, and Hulsbosch 1979).

But even in the unlikely event that a compact gas cloud of sufficient mass did fall in, the tidal perturbations should have taken the form of *broad* fans of stars, because the velocity dispersion in massive spheroids is large (e.g., Schechter and Gunn 1979). Such tidal fans are seen, e.g., in the interacting D galaxies NGC 7236 and 7237 that form Arp 169, in Arp 171, Arp 167, and IC 5250. Why then are the loops in NGC 1316 so much narrower?

One first hypothesis is that buried in the spheroid there existed a weak disk that was recently perturbed by a passing galaxy. Because of the presumably low velocity dispersion of that disk, the latter responded to the gravitational impulse with narrow tides of the kind modeled by Pfleiderer (1963), Clutton-Brock (1972), Toomre and Toomre (1972), and various others.

However, this hypothesis seems doomed for lack of a good candidate perturber near NGC 1316. The only nearby companion of considerable mass is NGC 1317,

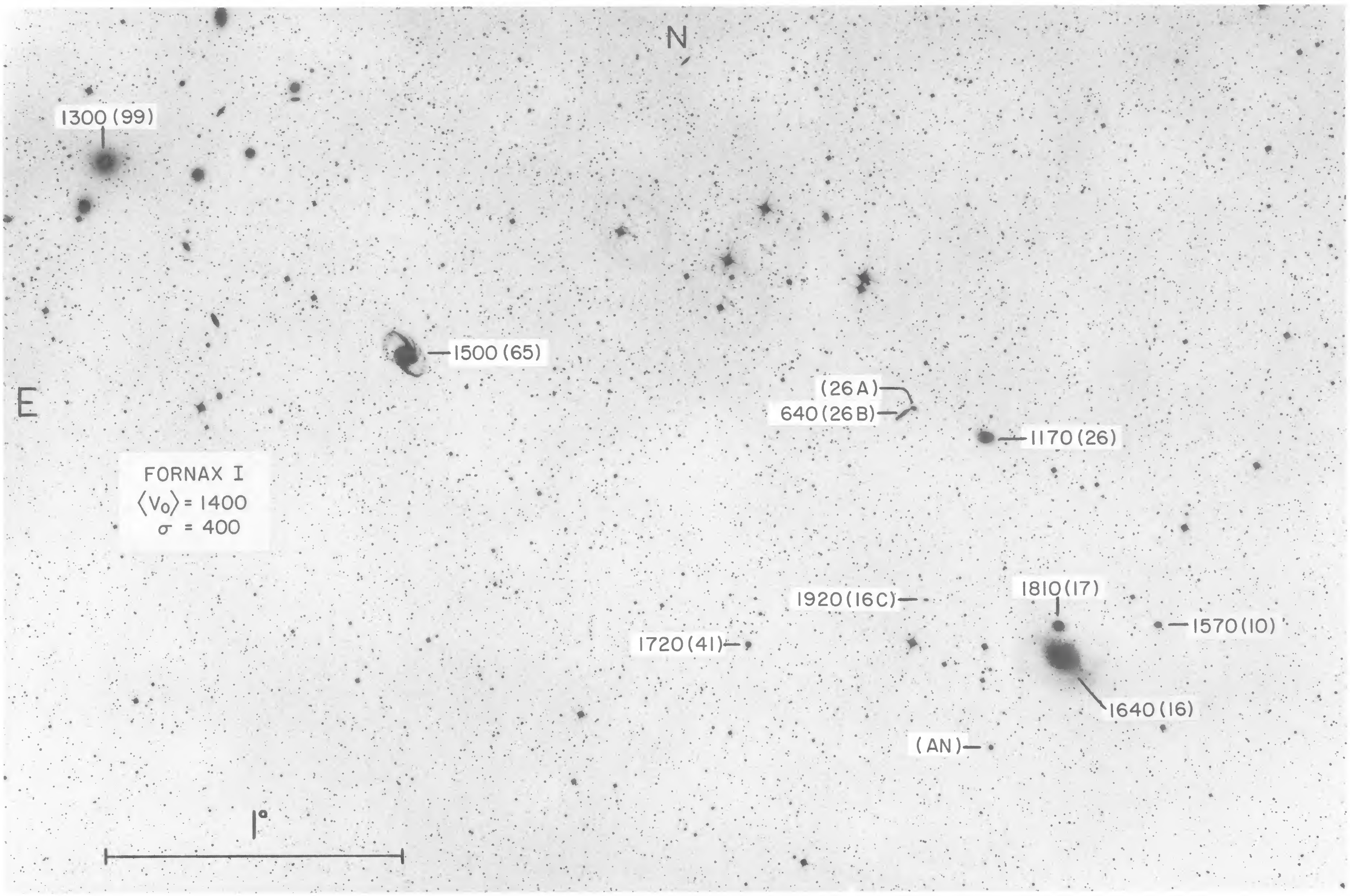

FIG. 15.—Galaxies around NGC 1316. The first attached number gives the radial velocity relative to the Local Group (rounded to 10 km s^{-1}; from the 2RC, Sandage 1978, and unpublished measurements), whereas the digits in parentheses give the NGC number when added to 1300. The bright galaxy to the lower right is NGC 1316 itself (v_{LG} = 1640 km s^{-1}); the galaxies around NGC 1399 (*upper left*) form the core of the Fornax I cluster.

which lies at a projected distance of 6'.3 (60 kpc) and has a similar radial velocity (Fig. 15). Yet NGC 1317 looks so regular and unperturbed (§ III*e*) that it appears to be an unlikely candidate; after all, if it were the culprit, it should have been severely damaged by the 8 times more luminous (and massive) NGC 1316. Among the more distant companions, NGC 1326 is about as bright as NGC 1317, but seems both too distant (47' = 450 kpc) and too fast ($\Delta v = 470$ km s^{-1}) to have caused much damage, if ever it passed near NGC 1316. Of the three remaining, nearer companions, NGC 1310, NGC 1316C, and the anonymous galaxy 23' SE, none appears massive enough to even be suspect. Thus, since the perturber of NGC 1316 is nowhere to be found, we are led to the new hypothesis that it probably fell in.

A strong hint that at least one galaxy *did* fall in is provided by the great extent of loop L_2, which stretches over ~10' (100 kpc) before connecting to ripple R_2 (§ III*a*). Long filaments of this sort frequently seem to be signatures of *strong* past tidal interactions.

Since NGC 1316 has at least two major loops, L_1 and L_2, one may even venture the guess that perhaps *two* galaxies fell in, the loops then being the remains of the tails. These would have reached their current extent in about 4–8 × 10^8 yr, if one assumes transverse tail velocities of 100–200 km s^{-1}. Such velocities are suggested by the radial velocities of typically 70–150 km s^{-1} observed in tails of interacting galaxies (Stockton 1974; Schweizer 1978; van der Hulst 1979).

The hypothesis that one or two galaxies fell in relieves us of an earlier embarrassment: for an outsider to have done the damage, we had to postulate the existence of a stellar disk in NGC 1316, yet no such disk is revealed by our photometry (§ IV*a*). Galaxy infall, on the other hand, supplies the loop material quite naturally in the form of debris from the intruder(s).

The idea that galaxies merge is, of course, not new (for reviews, see Ostriker 1977 and Toomre 1977). Early calculations by Alladin (1965) hinted already that colliding galaxies tend to stick. Later, Toomre and Toomre (1972) proposed specific objects from Arp's (1966) atlas as candidate mergers. Recent observations of the two-tailed NGC 7252 strongly suggest that, there, two disk galaxies have just completed merging (Schweizer 1978; and in preparation). In NGC 5128, too, the infall of a small galaxy may explain the rapid rotation of the disk and the presence of several, apparently stellar streamers in the spheroid (Graham 1979). Those streamers resemble the faint loops L_3 and L_4 of NGC 1316, but are even fainter. Since the time scale for diffusion of tidal filaments is at most a few times 10^8 years, the comparison suggests that NGC 5128 experienced infall slightly longer ago than NGC 1316.

Two objections against merging galaxies have often been raised, but seem invalid. One has most recently been expressed by Dufour *et al.* (1979), who believe that "the lack of an observed nucleus of the captured galaxy near NGC 5128 remains the greatest problem in accepting such a scenario." According to this view, the nucleus of the intruder ought to emerge from the debris and presumably continue on its orbit due to its compactness. However, there are both theoretical and observational arguments against this notion. The nucleus of any galaxy sits at the bottom of a potential well, where the escape velocity is typically 500–1000 km s^{-1} for a full-sized disk galaxy. Since the merging of two galaxies strongly depends on a slow initial approach velocity (at most a few hundred km s^{-1}), the nuclei can hardly make it out of their potential wells as long as the galaxies exist as separate entities. But even as the galaxies disintegrate, the nuclei cannot escape the now common potential well. Furthermore, they must spiral rapidly toward the new center since they experience strong decelerations due to dynamical friction (Chandrasekhar 1943), in amounts directly proportional to their masses (Tremaine, Ostriker, and Spitzer 1975). An observational survey of candidate mergers also shows that double nuclei with projected separations less than ~5 kpc are seen very rarely; this supports the notion that in the final stages the merging process is complete and rapid (Schweizer 1978).

A second objection concerns the color of NGC 1316: should increased star formation in a recent merger not make it rather blue? We can only guess that the color depends on many parameters, including the gas fraction and relative mass of each participant. Especially in the case that only one of the participants had significant amounts of gas, star formation need not have been strong. Also, if the merging took place several times 10^8 years ago, as indicated in NGC 1316 by the estimated expansion times of the loops, the stars that may have formed initially had sufficient time to redden significantly through evolution (Searle, Sargent, and Bagnuolo 1973; Larson and Tinsley 1978). We would scarcely be surprised if those knots near the center of NGC 1316 (§ III*d*) turned out to be clumps of stars formed in the merging process or, conceivably, former OB associations of the intruder.

Some special questions are raised by our discovery of the giant loop L_5 (§ III*a*), whose expansion time is of the order of 1–2 × 10^9 yr, if again we assume transverse velocities of 100–200 km s^{-1}. Thus, loop L_5 would seem to be significantly older than the loops within the envelope. Was it also formed by infall? Or, perhaps, by some long-past interaction with NGC 1317, or even with the now distant NGC 1365?

These questions make it amply clear that, although there exists a substantial amount of evidence in favor of NGC 1316 having accreted one or several neighbors within the last 4 × 10^8–2 × 10^9 yr, the exact circumstances remain obscure. Further progress will depend on a spectroscopic check that the loops indeed consist of stars and on detailed measurements of the loop velocities.

d) *Ripples*

The presence of ripples deep within NGC 1316 (§§ III*a* and IV*c*) may be yet another indication that a small galaxy fell in recently. In this view, the ripples represent a milder version of the strong response that occurs in the disk of a galaxy when an intruder of comparable mass free-falls through the center: a circular density wave runs outward, followed sometimes by minor waves, and gives the galaxy the appearance of a ring (Lynds and Toomre 1976; Toomre 1978).

The time scale for ripple formation can be estimated in classic fashion (e.g., Schwarzschild 1958) as the time τ it takes material at a radius r to react to a fractional change f of the gravitational force by moving a radial distance fr: $\tau \approx (2r^3/G\mathfrak{M}_r)^{1/2}$, where $\mathfrak{M}_r$ is the mass interior to r. At a radius of 25 kpc typical for the ripples in NGC 1316, $\tau \approx 6 \times 10^7$ yr (for $\mathfrak{M}/L_B = 10$). It may have taken a ripple a few τ's, or $2\text{–}6 \times 10^8$ yr, to travel over half the current radius under the influence of a small mass increment ($\sim$5–20%); this time interval is similar to the estimated expansion times of the loops.

As in the case of the loops, a possible difficulty with this interpretation is that narrow ripples are likely to form only in a disk and not in a spheroid. However, observations of other galaxies suggest that the debris of a merger may provide the material for ripple formation. Plates obtained of NGC 7252 in excellent seeing show several rings of delicate ripples; yet the light distribution in this wreck of two former disks (Schweizer 1978) is already well characterized by an $r^{1/4}$ law (unpublished result). Also among the five galaxies in Arp's (1966) category of "concentric rings" (Arp 227–231), Arp 230 has no companion, yet shows a superb set of ripples surrounding a central mess that betrays a recent struggle. These and other examples suggest that ripples tend to form in the general splatter produced by a merger.

Do other radio galaxies also have ripples? In NGC 5128, two possible ripples of extremely low contrast may be seen on the SRC(J) Sky Survey film about 8′ and 12′ northeast of the nucleus; each subtends $\sim$45°, and the outer one may have an even weaker counterpart to the southwest. M87 has no known ripples. (However, we have not had access to high-quality IIIa-J plates of this galaxy.) M89 (NGC 4552), on the other hand, has a beautiful set of ripples and a "jet...probably composed of stars" (Malin 1979). Malin comments: "Tidal interaction with another galaxy cannot be discounted as the disruptive force, but there seems to be no likely candidate in the vicinity, and that mechanism would not account for the active radio nucleus or the concentric shells." On the contrary, we would argue, that "jet" and the shells point to a recent merger which probably also fueled the nucleus.

In summary, the surprising number of galaxies with ripples *but no companions* fosters our belief that NGC 1316, too, has been shaken by a recent intruder rather than by any of the present neighbors. Especially the innermost, nonconcentric ripples (Fig. 2) indicate a so obviously short-lived disequilibrium that they *must* have formed recently.

e) *Fueling the Nucleus*

The two dust lanes which lead from distances of several kiloparsecs directly into the nucleus of NGC 1316 are probably spiral-shaped (§ III*b*). If they lie within the rotating gas disk, as seems likely, their orientation and relative visibility indicate that they trail. Trailing dust lanes that wind directly into the nucleus have long been known in certain spirals (e.g., in NGC 4321 and 5457 [Sandage 1961]), but here they are observed for the first time in the gas disk of a spheroidal galaxy.

Two conclusions can be drawn from the presence of these lanes. First, dust and (probably) associated cool gas survive in the ionized-gas disk of NGC 1316 to within small distances ($\lesssim 0\overset{''}{.}9$ [140 pc]) from the nucleus. Second, since dust lanes outline large-scale shocks in the gas (Fujimoto 1966; Roberts 1969; Mathewson, van der Kruit, and Brouw 1972) and shocks are dissipative, the disk gas must sink in further upon each passage through the shock, thus supplying fuel to the nucleus.

This fueling mechanism is probably several times more efficient than the cloud-drag mechanism studied by Gunn (1977), which already generates a mass influx of $1\ \mathfrak{M}_\odot\ \text{yr}^{-1}$. Thus, the inclined gas disk and central dust lanes of NGC 1316 provide supporting evidence for Shklovskii's (1962) suggestion that infall of a fresh supply of gas into the nucleus of a spheroidal galaxy may be responsible for subsequent radio outbursts. Because of the vast amount of gas still remaining in the disk reservoir ($\gtrsim 3 \times 10^8\ \mathfrak{M}_\odot$), it seems safe to predict that *further outbursts of NGC 1316 will occur*.

It is a pleasure to thank J. A. Graham for generously sharing his plates and knowledge with me, W. M. Goss and A. Toomre for helpful discussions and correspondence, C. Monsalve for excellent photographic work, and C. Aguirre for help with the data reduction.

REFERENCES

Aaronson, M., Cohen, J. G., Mould, J., and Malkan, M. 1978, *Ap. J.*, **223**, 824.
Albert, C. E., White, R. A., and Morgan, W. W. 1977, *Ap. J.*, **211**, 309.
Alladin, S. M. 1965, *Ap. J.*, **141**, 768.
Arp, H. 1964, *Ap. J.*, **139**, 1378.
———. 1966, *Atlas of Peculiar Galaxies* (Pasadena: California Institute of Technology).
Baade, W., and Minkowski, R. 1954, *Observatory*, **74**, 130.
Bottinelli, L., and Gouguenheim, L. 1978, *Astr. Ap.*, **64**, L3.
Burbidge, E. M., and Burbidge, G. R. 1959, *Ap. J.*, **129**, 271.
Burbidge, G. R., Burbidge, E. M., and Sandage, A. R. 1963, *Rev. Mod. Phys.*, **35**, 947.
Burkhead, M. S. 1978, *Ap. J. Suppl.*, **38**, 147.
Cameron, M. J. 1971, *M.N.R.A.S.*, **152**, 439.
Chandrasekhar, S. 1943, *Ap. J.*, **97**, 255.
Clutton-Brock, M. 1972, *Ap. Space Sci.*, **17**, 292.
Crawford, D. L., Golson, J. C., and Landolt, A. U. 1971, *Pub. A.S.P.*, **83**, 652.
de Vaucouleurs, G. 1953*a*, *M.N.R.A.S.*, **113**, 134.

de Vaucouleurs, G. 1953*b*, *Observatory*, **73**, 252.
———. 1959, in *Handbuch der Physik*, Vol. **53**, ed. S. Flügge (Berlin: Springer), p. 311.
———. 1974, in *IAU Symposium 58, The Formation and Dynamics of Galaxies*, ed. J. R. Shakeshaft (Dordrecht: Reidel), p. 335.
———. 1975, in *Galaxies and the Universe*, ed. A. Sandage, M. Sandage, and J. Kristian (Chicago: University of Chicago Press), p. 557.
de Vaucouleurs, G., and Capaccioli, M. 1979, *Ap. J. Suppl.*, **40**, 699.
de Vaucouleurs, G. and de Vaucouleurs, A. 1972, *Mem. R.A.S.*, **77**, 1.
de Vaucouleurs, G., de Vaucouleurs, A., and Corwin, H. G. 1976, *Second Reference Catalogue of Bright Galaxies* (Austin: University of Texas Press) (2RC).
Dufour, R. J., van den Bergh, S., Harvel, C. A., Martins, D. H., Schiffer, F. H., Talbot, R. J., Talent, D. L., and Wells, D. C. 1979, *A.J.*, **84**, 284.
Evans, D. S. 1949, *M.N.R.A.S.*, **109**, 94.
Fosbury, R. A. E., Mebold, U., Goss, W. M., and Dopita, M. A. 1978, *M.N.R.A.S.*, **183**, 549.
Freeman, K. C. 1970, *Ap. J.*, **160**, 811.
Fujimoto, M. 1966, in *IAU Symposium 29, Nonstable Phenomena in Galaxies*, ed. M. Arekeljan (Yerevan: Armenian Academy of Science), p. 435.
Gardner, F. F., and Whiteoak, J. B. 1971, *Australian J. Phys.*, **24**, 899.
Geldzahler, B. J., and Fomalont, E. B. 1978, *A.J.*, **83**, 1047.
Graham, J. A. 1979, *Ap. J.*, **231**, 60.
Gunn, J. E. 1977, "Feeding the Monster: Gas Disks in Elliptical Galaxies," presented at NATO Conference "Energy Sources and Emission Mechanisms in QSOs," Cambridge.
Heiles, C. 1976, *Ap. J.*, **204**, 379.
Hodge, P. W. 1975, *Sky Tel.*, **49**, 354.
Hubble, E. 1923, *Pub. A.S.P.*, **35**, 261.
Jenkins, E. B., and Savage, B. D. 1974, *Ap. J.*, **187**, 243.
King, I. R. 1978, *Ap. J.*, **222**, 1.
Knapp, G. R., Faber, S. M., and Gallagher, J. S. 1978, *A.J.*, **83**, 11.
Knapp, G. R., Gallagher, J. S., and Faber, S. M. 1978, *A.J.*, **83**, 139.
Knapp, G. R., and Kerr, F. J. 1974, *Astr. Ap.*, **35**, 361.
Knapp, G. R., Kerr, F. J., and Williams, B. A. 1978, *Ap. J.*, **222**, 800.
Kormendy, J. 1977, *Ap. J.*, **218**, 333.
Kotanyi, C. G., and Ekers, R. D. 1979, *Astr. Ap.*, **73**, L1.
Kunkel, W. E., and Rydgren, A. E. 1979, *A.J.*, **84**, 633.
Landolt, A. U. 1973, *A.J.*, **78**, 959.
Larson, R. B., and Tinsley, B. M. 1978, *Ap. J.*, **219**, 46.
Lockhart, I. A. 1971, Ph.D. thesis, Australian National University, Canberra.
Lynds, R., and Toomre, A. 1976, *Ap. J.*, **209**, 382.
Malin, D. F. 1977, *AAS Photo-Bull.* No. 16, p. 14.
———. 1979, *Nature*, **277**, 279.
Materne, J., Huchtmeier, W. K., and Hulsbosch, A. N. M. 1979, *M.N.R.A.S.*, **186**, 563.
Mathewson, D. S., van der Kruit, P. C., and Brouw, W. N. 1972, *Astr. Ap.*, **17**, 468.
Matthews, T. A., Morgan, W. W., and Schmidt, M. 1964, *Ap. J.*, **140**, 35.
Mees, C. E. K., and James, F. H. 1966, *The Theory of the Photographic Process* (3d ed.; New York: Macmillan), p. 495.
Mills, B. Y. 1954, *Observatory*, **74**, 248.
Moffet, A. T. 1975, in *Galaxies and the Universe*, ed. A. Sandage, M. Sandage, and J. Kristian (Chicago: University of Chicago Press), p. 211.
Morgan, W. W., Kayser, S., and White, R. A. 1975, *Ap. J.*, **199**, 545.
Oemler, A. 1973, *Ap. J.*, **180**, 11.
———. 1976, *Ap. J.*, **209**, 693.
Osterbrock, D. E. 1974, *Astrophysics of Gaseous Nebulae* (San Francisco: Freeman), p. 65.
Ostriker, J. P. 1977, in *Evolution of Galaxies and Stellar Populations*, ed. R. B. Larson and B. M. Tinsley (New Haven: Yale University Observatory), p. 369.
Patterson, F. S. 1940, *Harvard College Obs. Bull.*, No. 914, 9.
Pfleiderer, J. 1963, *Zs. Ap.*, **58**, 12.
Racine, R., Oke, J. B., and Searle, L. 1978, *Ap. J.*, **223**, 82.
Reif, K., Mebold, M., and Goss, W. M. 1978, *Astr. Ap.*, **67**, L1.
Roberts, W. W. 1969, *Ap. J.*, **158**, 123.
Sandage, A. 1961, *The Hubble Atlas of Galaxies* (Washington: Carnegie Institution of Washington).
———. 1972*a*, *Ap. J.*, **176**, 21.
———. 1972*b*, *Ap. J.*, **178**, 1.
———. 1978, *A.J.*, **83**, 904.
Sandage, A., and Tammann, G. A. 1976, *Ap. J.*, **210**, 7.
Sandage, A., and Visvanathan, N. 1978, *Ap. J.*, **223**, 707.
Sargent, W. L. W. 1977, in *Evolution of Galaxies and Stellar Populations*, ed. R. B. Larson and B. M. Tinsley (New Haven: Yale University Observatory), p. 427.
Schechter, P. L., and Gunn, J. E. 1978, *A.J.*, **83**, 1360.
———. 1979, *Ap. J.*, **229**, 472.
Schild, R., and Davis, M. 1979, *A.J.*, **84**, 311.
Schild, R., and Oke, J. B. 1971, *Ap. J.*, **169**, 209.
Schwarzschild, M. 1958, *Structure and Evolution of the Stars* (Princeton: Princeton University Press), p. 30.
Schweizer, F. 1978, in *IAU Symposium No. 77, Structure and Properties of Nearby Galaxies*, ed. E. M. Berkhuijsen and R. Wielebinski (Dordrecht: Reidel), p. 279.
———. 1979, *Ap. J.*, **233**, 23.
———. 1980, in preparation.
Searle, L. 1965, *Nature*, **207**, 1282.
Searle, L., Sargent, W. L. W., and Bagnuolo, W. G. 1973, *Ap. J.*, **179**, 427.
Sérsic, J. L. 1968, *Atlas de Galaxias Australes* (Cordoba: Universidad Nacional de Cordoba), p. 87.
Shane, W. W. 1977, *Bull. AAS*, **9**, 362.
Shklovskii, I. S. 1962, *Soviet Astr.—AJ*, **6**, 465.
Shklovskii, I. S., and Cholopov, P. N. 1952, *Astr. Circ. Acad. Sci. USSR*, No. 131, p. 2.
Stanley, G. J., and Slee, O. B. 1950, *Australian J. Sci. Res.*, *A*, **3**, 234.
Stockton, A. 1974, *Ap. J.*, **187**, 219.
Strom, S. E., and Strom, K. M. 1978, *A.J.*, **83**, 732.
Strom, S. E., Strom, K. M., Goad, J. W., Vrba, F. J., and Rice, W. 1976, *Ap. J.*, **204**, 684.
Toomre, A. 1977, in *Evolution of Galaxies and Stellar Populations*, ed. R. B. Larson and B. M. Tinsley (New Haven: Yale University Observatory), p. 401.
———. 1978, in *IAU Symposium No. 79, The Large Scale Structure of the Universe*, ed. M. S. Longair and J. Einasto (Dordrecht: Reidel), p. 109.
Toomre, A., and Toomre, J. 1972, *Ap. J.*, **178**, 623.
Tremaine, S. D., Ostriker, J. P., and Spitzer, L. 1975, *Ap. J.*, **196**, 407.
Ulrich, M.-H. 1975, *Pub. A.S.P.*, **87**, 965.
van den Bergh, S. 1969, *Ap. J. Suppl.*, **19**, 145.
van der Hulst, J. M. 1979, *Astr. Ap.*, **71**, 131.
Wade, C. M. 1961, *Pub. N.R.A.O.*, **1**, 99.
Welch, G. A., Chincarini, G., and Rood, H. J. 1975, *A.J.*, **80**, 77.
Whitford, A. E. 1971, *Ap. J.*, **169**, 215.
Young, P. J., Westphal, J. A., Kristian, J., Wilson, C. P., and Landauer, F. P. 1978, *Ap. J.*, **221**, 721.
Zwicky, F. 1959, in *Handbuch der Physik*, Vol. **53**, ed. S. Flügge (Berlin: Springer), p. 390.

FRANÇOIS SCHWEIZER: Cerro Tololo Inter-American Observatory, Casilla 63-D, La Serena, Chile

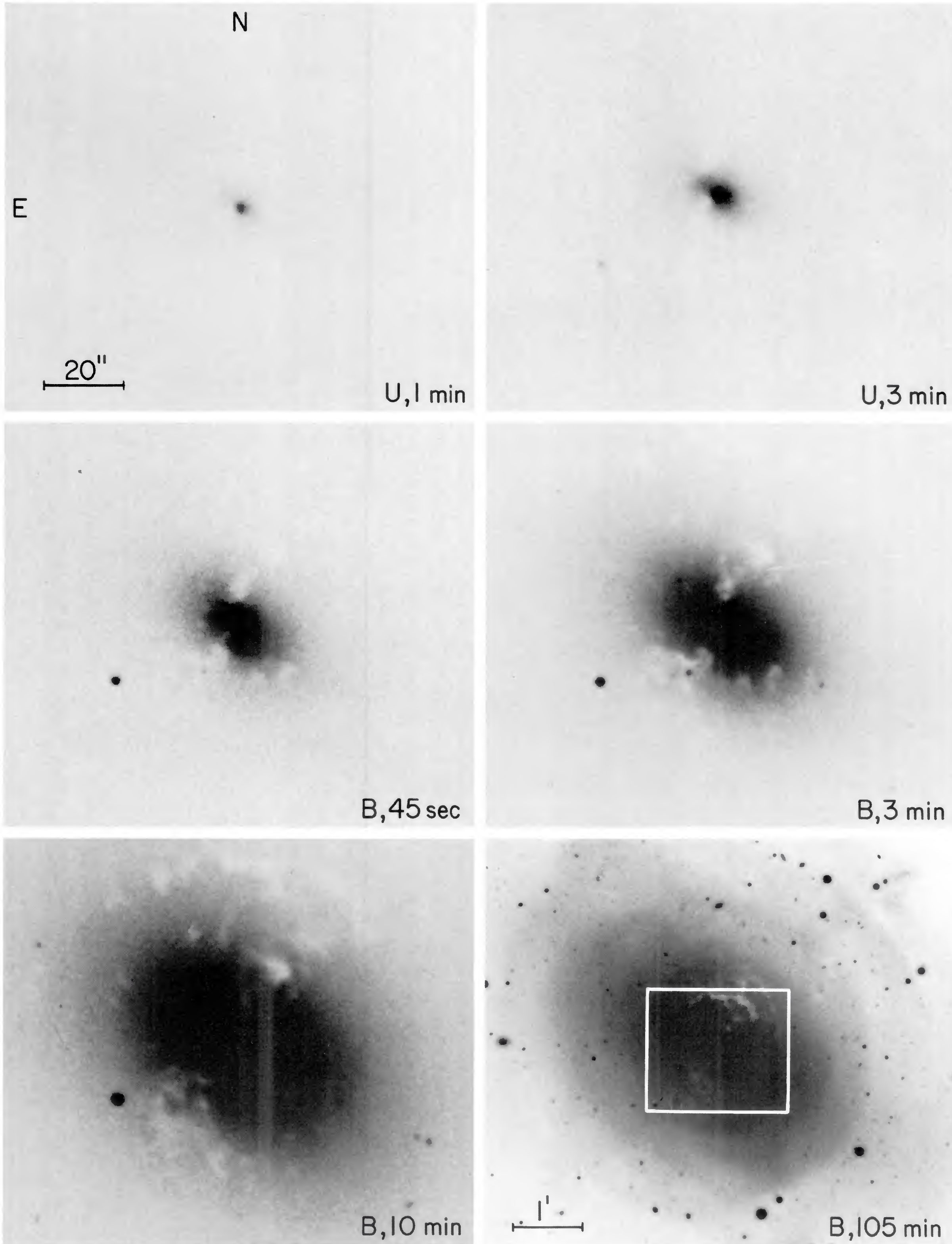

FIG. 3.—Six photographs of increasing exposure showing the nucleus, spheroid, and dust patches of NGC 1316; reproduced from ultraviolet (U: IIIa-J + UG − 1) and blue (*B*: IIIa-J + GG − 385) plates obtained at the 4 m prime focus in 1″ seeing. The first five photographs are on a uniform scale (20″ bar in top left frame) and cover the field framed in white in the sixth, smaller-scale photograph (*bottom right*).

SCHWEIZER (*see* page 304)

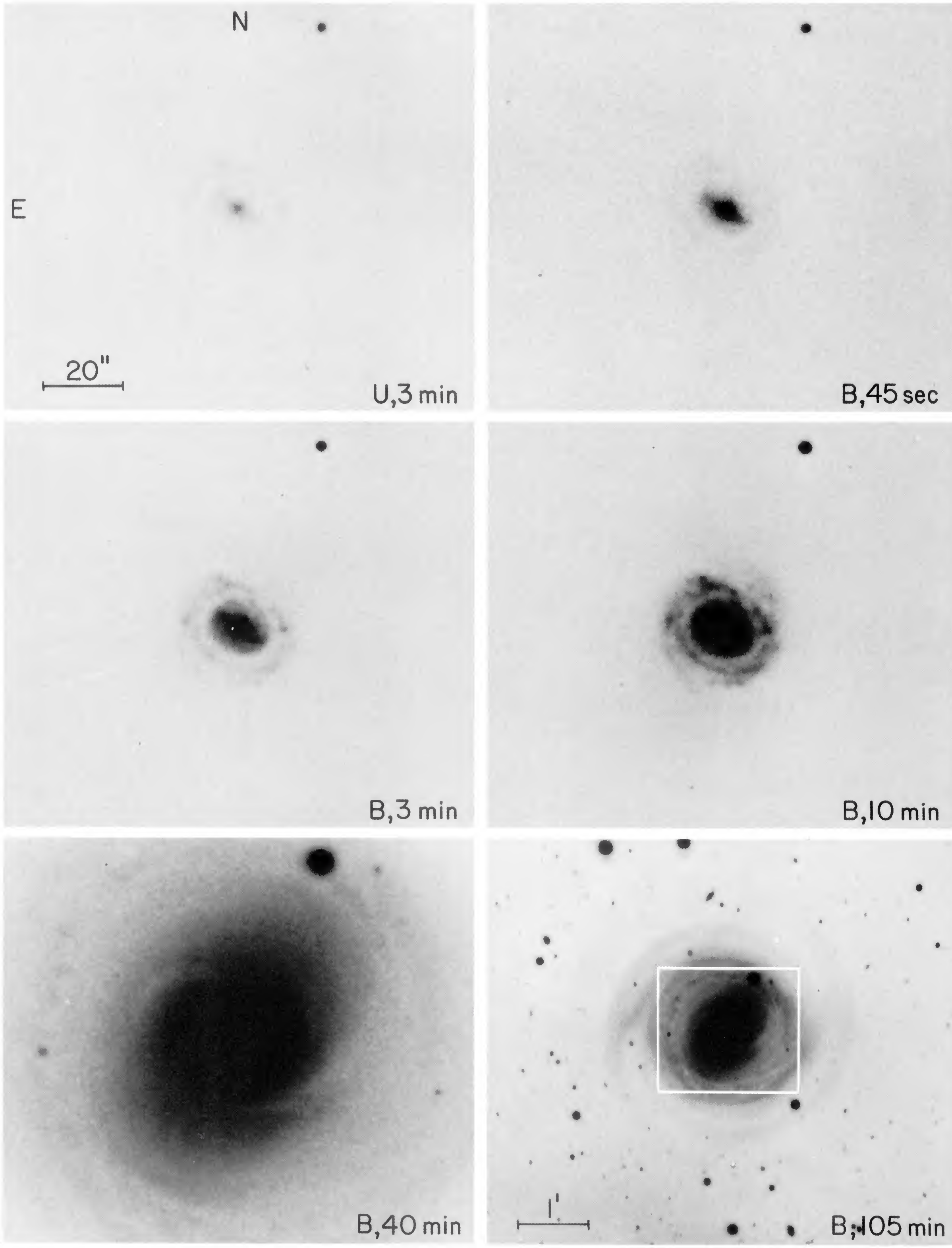

FIG. 4.—Six photographs of NGC 1317, the companion galaxy of NGC 1316, showing the nucleus, central bar, ring of H II regions, "fat" bar, and spiral structure. (Five of the six photographs are reproduced from the same plates as the photographs in Fig. 3.) Note that the "fat" bar appears perpendicular to the smaller, central bar.

SCHWEIZER (*see* page 304)

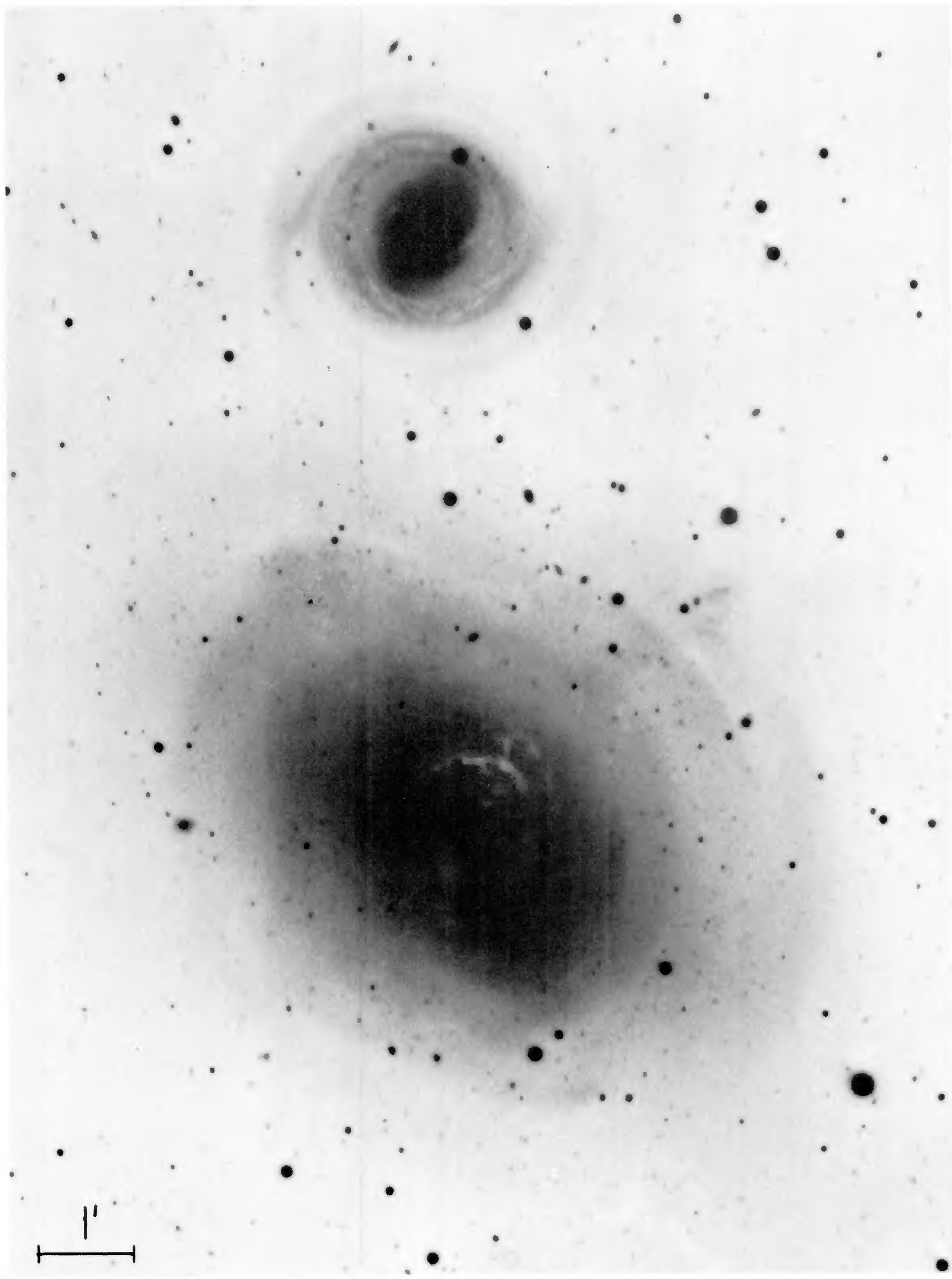

FIG. 5.—Dodged photograph of NGC 1316/1317 showing the ripples and plume in the spheroid of NGC 1316 (cf. with Fig. 2); reproduced from plate P-3411 (4 m prime focus, baked IIIa-J + GG − 385, 105 min exposure, 1″.5 seeing) by the technique of unsharp masking, which reduces large-scale contrast while preserving small-scale contrast (Mees and James 1966; Malin 1977).

SCHWEIZER (*see* page 304)

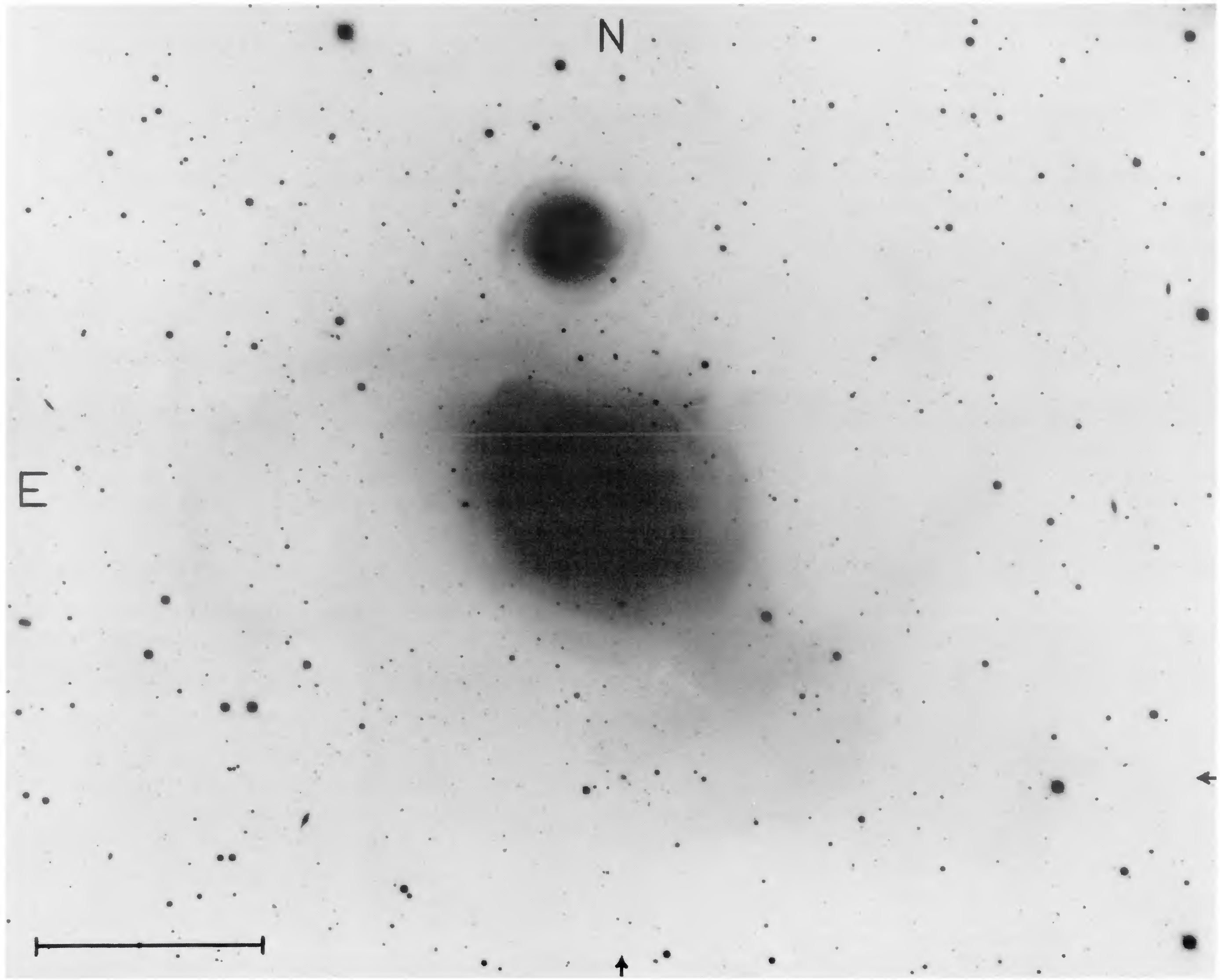

FIG. 6.—Photograph of NGC 1316/1317 showing the relation between the spheroid of NGC 1316, the ripples, and the loops (from same plate as Fig. 5). Note the faint arc that connects L_2 and R_2, and the dust lane NW of the only detected H II region(*arrows*; cf. with Fig. 2). The scale bar is 316″ (50 kpc).

SCHWEIZER (*see* page 304)

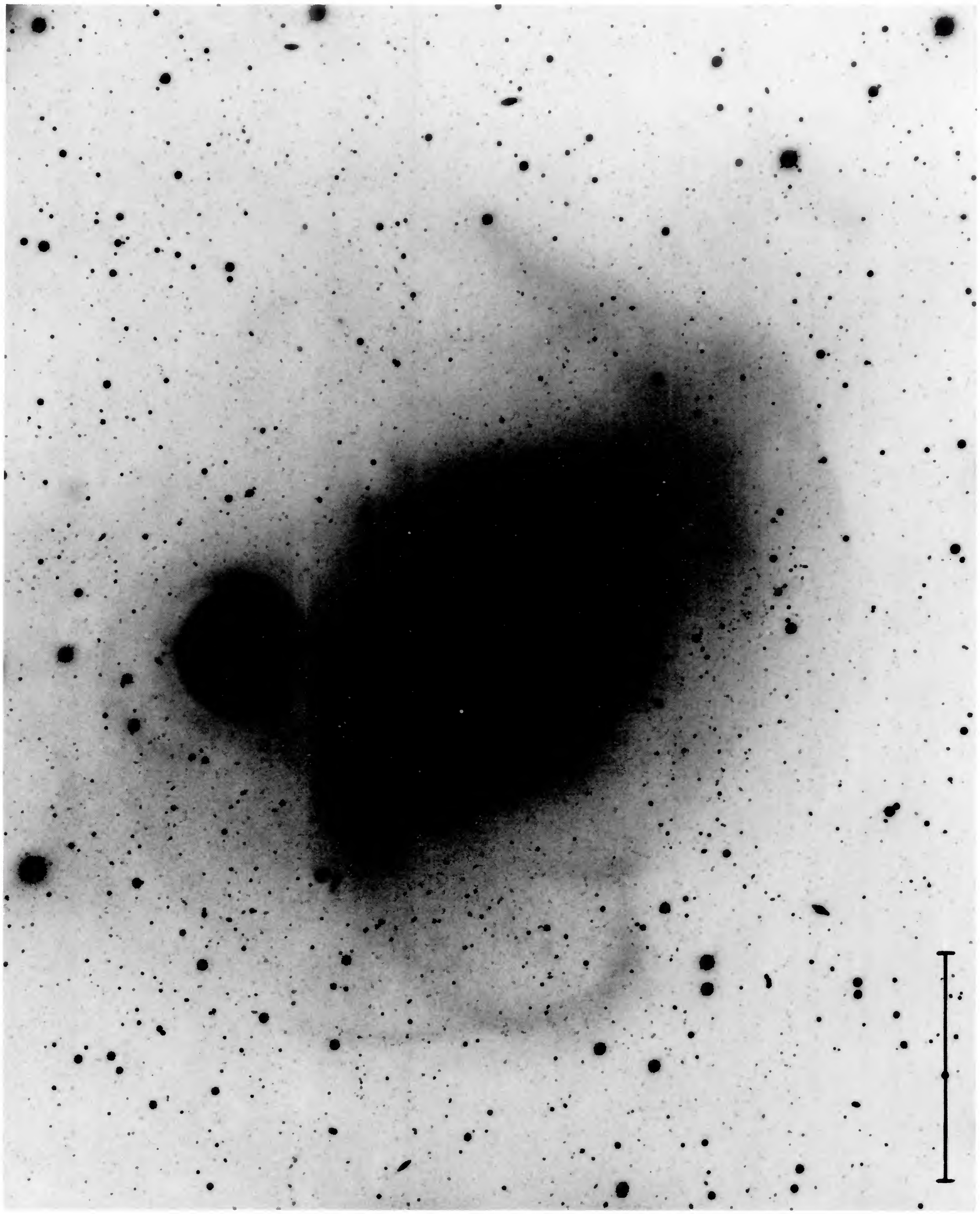

FIG. 7.—High-contrast photograph showing the loops and envelope of NGC 1316 (made from same plate as Fig. 5). The scale bar is 316″ (50 kpc), and the field shown is the same as in Fig. 6.

SCHWEIZER (*see* page 304)

FIG. 8.—High-contrast photograph of a 41′ × 50′ field centered on NGC 1316/1317 (same plate as in Fig. 5). Notice the vast luminous envelope that is characteristic of D galaxies; its projected size is at least 19′ × 23′ (180 × 220 kpc). The faintest light levels seen on this reproduction correspond to $B \approx 27$ mag arcsec^{-2}.

SCHWEIZER (*see* page 304)

1980ApJ...237..303S

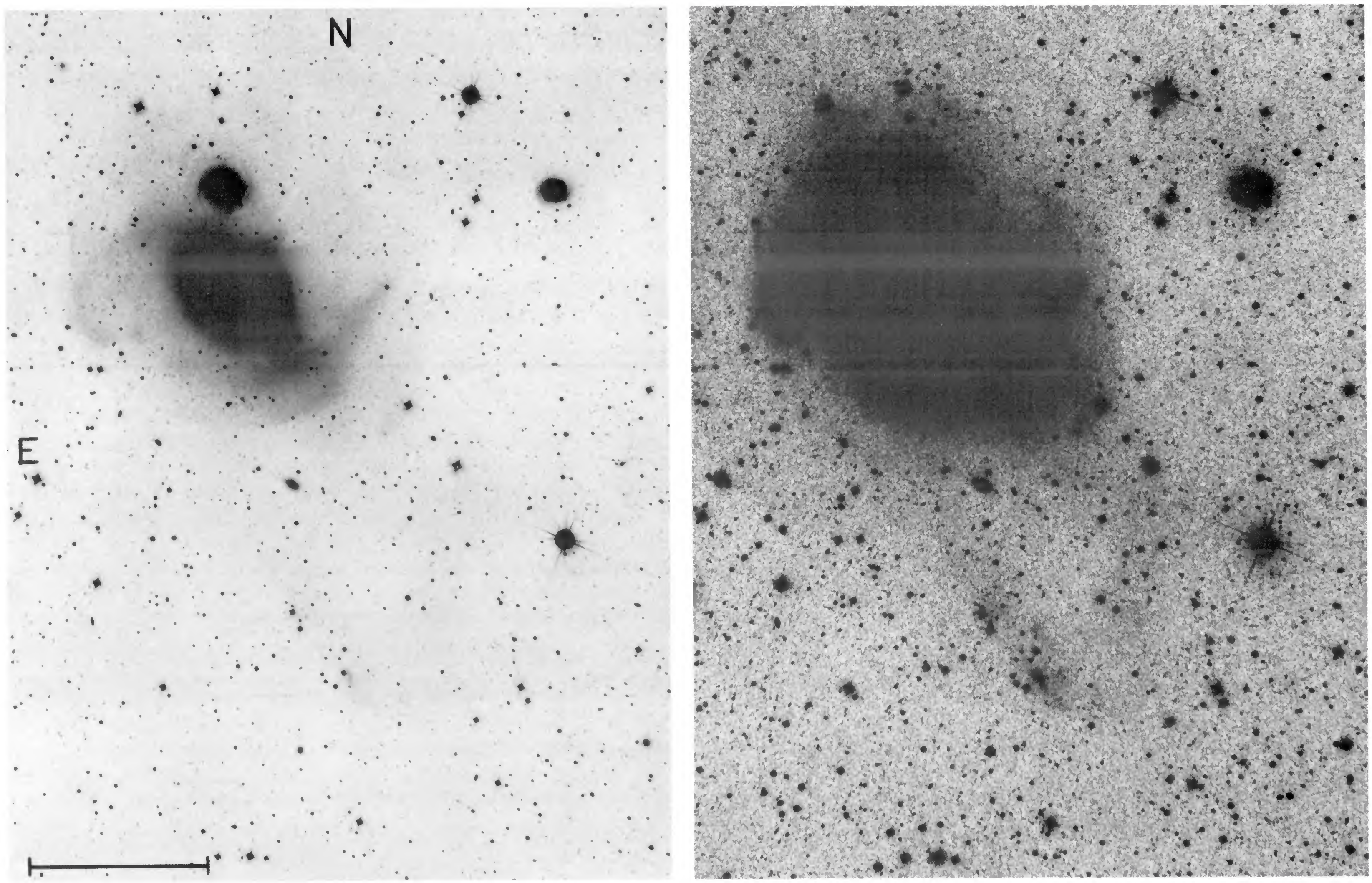

FIG. 9.—Integration prints of five Curtis Schmidt plates (baked IIIa-J + GG-385, exposed ~3 hr each) showing the giant loop L_5 protruding from the envelope to the south-southwest. The left and right frames are low- and high-contrast integrations of the same five plates. The scale bar measures 10′.5 (100 kpc). Comparison with Fig. 10 shows that most of the loop lies outside the radio lobes.

SCHWEIZER (*see* page 304)

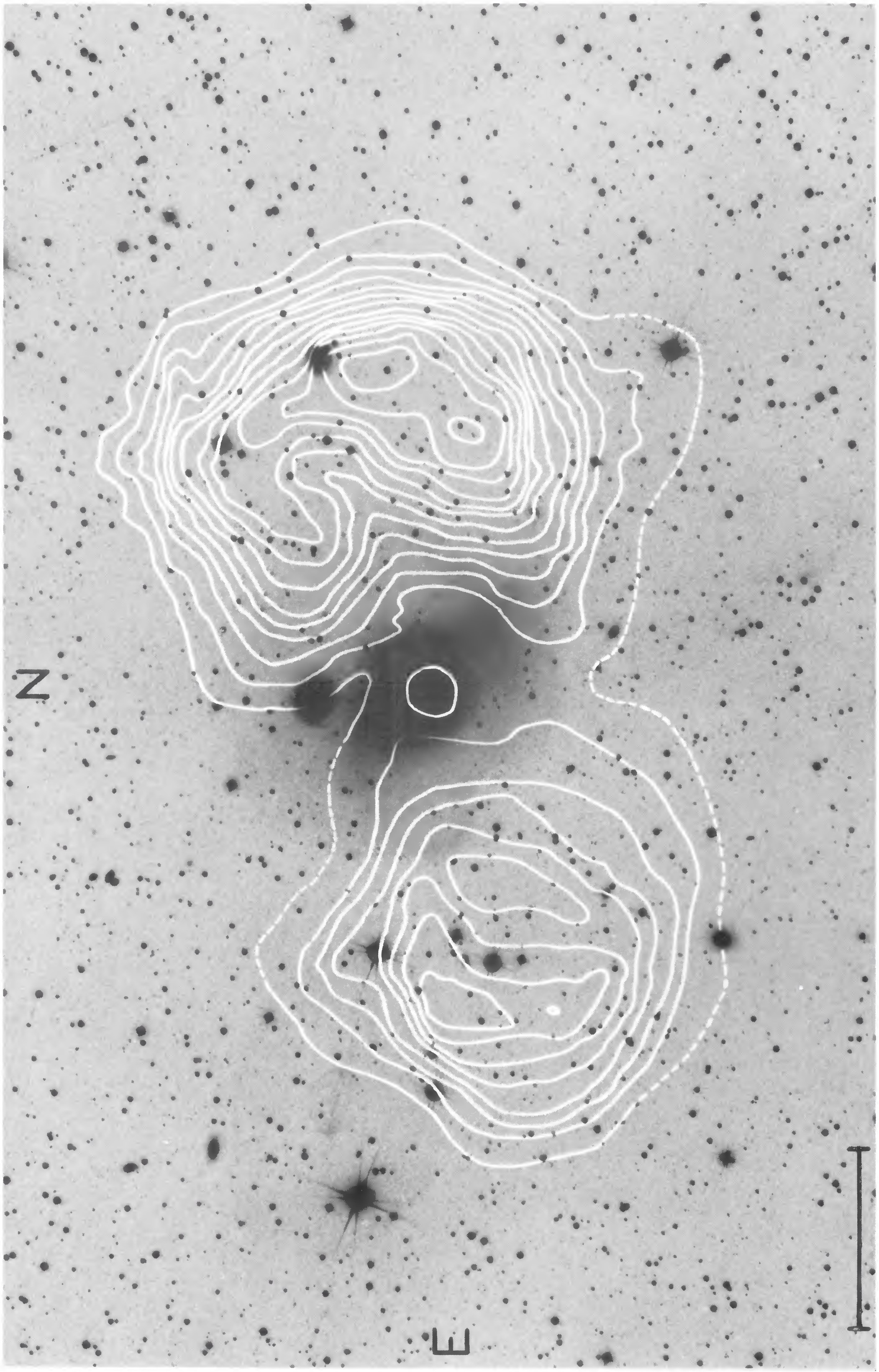

FIG. 10.—Cameron's (1971) radio map of Fornax A superposed on a photograph of NGC 1316. The contours of 73.5 cm (408 MHz) continuum radiation are in units of 10^4 K. The scale bar measures 10'.5 (100 kpc). (No attempt has been made to correct the radio map for its 7% scale difference between R.A. [larger] and decl. [smaller]; the mean radio scale is equal to the scale of the photograph.) Note the nuclear source and the steep outer gradient of the western lobe.

SCHWEIZER (*see* page 304)